COMPARATIVE STUDY OF DIFFERENT HONEYCOMB GEOMETRIES FOR THE SUPPRESSION OF CONVECTIVE HEAT TRANSFER IN FLAT PLATE SOLAR COLLECTORS

BY

SANUSI, YINKA SOFIHULLAHI B.Sc (Unilorin 2003)

(M.Sc/ENG/03229/06-07)

M.Sc. THESIS SUBMITTED TO THE

POSTGRADUATE SCHOOL

AHMADU BELLO UNIVERSITY, ZARIA

NIGERIA

IN PARTIAL FULFILMENT FOR THE AWARD OF MASTER OF SCIENCE IN MECHANICAL ENGINEERING

DEPARTMENT OF MECHANICAL ENGINEERING

AHMADU BELLO UNIVERSITY, ZARIA

NIGERIA

FEBRUARY, 2009

DECLARATION

I declare that the work in the thesis entitled **COMPARATIVE STUDY OF DIFFERENT HONEYCOMB GEOMETRIES FOR THE SUPPRESSION OF CONVECTIVE HEAT TRANSFER IN FLAT PLATE SOLAR COLLECTORS** has been performed by me in the Department of Mechanical Engineering under the supervision of Professor C.O.Folayan. The information derived from the literature has been duly acknowledged in the text and a list of references provided. No part of this thesis was previously presented for another degree or diploma at any university.

---------- ---------- ----------

SANUSI YINKA SOFIHULLAHI SIGNATURE DATE

CERTIFICATION

This thesis entitled **COMPARATIVE STUDY OF DIFFERENT HONEYCOMB GEOMETRIES FOR THE SUPPRESSION OF CONVECTIVE HEAT TRANSFER IN FLAT PLATE SOLAR COLLECTORS** by SANUSI, Yinka Sofihullahi meets the regulations governing the award of the degree of master of science of Ahmadu Bello University, Zaria, and is approved for its contribution to knowledge and literary presentation.

_____ _____

Chairman, Supervisory Committee **Date**

Professor C.O. Folayan

_____ _____

Member, supervisory Committee **Date**

Dr D.S. Yawas

_____ _____

Head of Department **Date**

Professor C.O. Folayan

_____ _____

Dean, Postgraduate School **Date**

Professor N.S. Nkom

DEDICATION

This thesis is dedicated to Almighty Allah for sparing my life and to my wife Bilikis and my son Abdulsalam for their love and affection

ACKNOWLEDGEMENT

I am indeed grateful to Almighty Allah who allowed me to go this far .I am thankful to him for his love, the blessing he bestowed on me on my chosen career and the successes he has made me to achieve so far.

I wish to express my profound gratitude to my supervisor Professor C .O. Folayan who contributed immensely to the success of the master program and this research work specifically. May almighty God continue to bless you with sound health and wisdom (Amen).

My appreciation also goes to the postgraduate coordinator Dr D.S. Yawas for his efficient coordination of the master's program and his advice at various stages of this work.

Special appreciation to my lecturers Engr. (Mrs.) R.B.O. Suleiman, Engr. F.O.Anafi, Dr. G.Y.Pam, Professor P.B. Madakson, Dr. A.I.Obi for their contribution during the course of the program.

I also wish to thank my senior colleagues Professor M.S.Abolarin, Engr. S.K. Laminu, Engr. D.M. Kulla, Engr. A.A. Alabi, Engr. M.O. Afolayan, Engr. Jumare Engr. S. Malachy, Dr. M. Dauda for their useful suggestions during this research work and presentations.

My sincere and hearty gratitude goes to my parents Alhaji Salman Sanusi and Alhaja Kuburat Sanusi for their unflinching moral and financial support to me and my family. May Almighty Allah continue to bless you and grant you long life with sound health (Amin).

Due regards to my brothers and sisters Kamilu, Abdullateef, Funke, Sahadat, Dupe, Rabiu, brother Muideen, Daddy Abddulrahaman and family, Daddy Rasaq and family, Hajia Mumin Olokunbi and family, Mummy Taofiq and family, Mummy Abolore and family Mummy Yetunde and family as well as the entire Sanusi Family for their kind gestures towards me. May Almighty Allah bless you all (Amin).

This program was splendid with the team work of my class mates Ojodale Sunday, Bashir Kunya, Tukur Yunusa and Mohammed Muazu. You people are great and committed team.

ABSTRACT

The performance of different honeycomb geometries have been compared experimentally in four identical solar water heaters equipped with circular, square and rectangular cell honeycomb structures while the fourth solar water heater was without honeycomb. The collector with circular, square and rectangular honeycomb collected 19.32%, 9.78% and3.0% more energy respectively when compared with collector without honeycomb. The overall analysis gave average exergetic efficiency of 48.8%, 44.9% and 42.1% for collector with circular, square and rectangular cell honeycomb respectively while the collector without honeycomb has an average exergetic efficiency of 40.9%

TABLE OF CONTENTS

Declaration ii

Certification iii

Dedication iv

Acknowledgements v

Abstract vii

Table of Contents viii

List of Figures xi

List of Plates xiii

List of Appendices xiv

List of Symbols xv

CHAPTER ONE

INTRODUCTION

1.1 Introduction 1

1.2 Statement of the Problem 3

1.3 Objective of the Study 4

1.4 Justification of the Study 4

CHAPTER TWO

LITERATURE REVIEW

2.1 Flat Plate Solar Collector 5

2.2 Absorber Plate 6

2.3 Cover Sheets 8

2.4 Solar Water Heating 9

2.5 Honeycomb Cell 12

2.6 Review of Past Work 17

2.7 Conclusion of the Review of Literature 20

CHAPTER THREE

DESIGN THEORY AND CALCULATIONS

3.1 Design Theory 21

3.2 Evaluation of the Overall Loss Coefficient (U_l) 21

3.3 Heat Removal Factor 24

3.4 Absorbed Solar Radiation(S) 24

3.5 Collector Performance 27

3.6 Calculation of the Hourly Radiation 27

3.7 Honeycomb Design 28

3.8 Design Calculations 28

CHAPTER FOUR

CONSTRUCTION, TESTING AND RESULT

4.1 Introduction 43

4.2 Construction Processes 43

4.3 Assembly of component parts 47

4.4 Description of the Experimental Set-Up 49

4.5 Experimentation 53

4.6 Result and Discussion 54

CHAPTER FIVE

SUMMARY, CONCLUSION AND RECOMMENDATION

5.1 Summary 71

5.2 Conclusion 72

5.3 Recommendation 73

References 74

LIST OF FIGURES

Page

Figure1.1: Various heat losses from the absorber to the ambient 2

Figure1.2: Schematic diagram of a square cell honeycomb 3

Figure2.1: The common arrangement of a flat plate solar collector 5

Figure2.2: A passive solar water heater 10

Figure 2.3: An Active solar water heater 11

Figure2.4: Continuous flow solar water heater 12

Figure2.5: Light transmittance in a square cell honeycomb 13

Figure 2.6a: Side view of a two dimensional honeycomb 13

Figure 2.6b: Plan view of a two dimensional honeycomb 14

Figure2.7: Variation of convective heat loss with increasing temperature difference for a honeycomb 15

Figure 3.1: The thermal analysis of a single cover flat plate solar collector 22

Figure3.2: The equivalent circuits of the thermal analysis of a single cover flat plate solar collector 22

Figure4.1: Flow diagram of the experimental set-up 50

Figure 4.2: Graph of the Rayleigh number against the local time for day1 55

Figure 4.3: Graph of the Nusselt number against the local time for day1 56

Figure 4.4: Graph of the Convective heat transfer coefficient against the local time for day1 56

Figure 4.5: Graph of the Useful heat output against the local time for day1 57

Figure 4.6: Graph of the Thermal efficiency against the local time for day1 58

Figure 4.7: Graph of the Exergetic efficiency against the local time for day1 58

Figure 4.8: Graph of the Rayleigh number against the local time for day2 59

Figure 4.9: Graph of the Nusselt number against the local time for day2 60

Figure 4.10: Graph of the Convective heat transfer coefficient against the local time for day2 60

Figure 4.11: Graph of the Useful heat output against the local time for day2 61

Figure 4.12: Graph of the Thermal efficiency against the local time for day2 61

Figure 4.13: Graph of the Exergetic efficiency against the local time for day2 62

Figure 4.14: Graph of the Rayleigh number against the local time for day3 63

Figure 4.15: Graph of the Nusselt number against the local time for day3 64

Figure 4.16: Graph of the Convective heat transfer coefficient against the local time for day3 64

Figure 4.17: Graph of the Useful heat output against the local time for day3 65

Figure 4.18: Graph of the Thermal efficiency against the local time for day3 65

Figure 4.19: Graph of the Exergetic efficiency against the local time for day3 66

Figure 4.20: Graph of the Rayleigh number against the local time for day4 67

Figure 4.21: Graph of the Nusselt number against the local time for day4 68

Figure 4.22: Graph of the Convective heat transfer coefficient against the local time for day4 68

Figure 4.23: Graph of the Useful heat output against the local time for day4 69

Figure 4.24: Graph of the Thermal efficiency against the local time for day4 69

Figure 4.25: Graph of the Exergetic efficiency against the local time for day4 70

LIST OF PLATES

Page

Plate 4.1: Front view of the experimental set-up 51

Plate 4.2: Side view of the experimental set-up 51

Plate4.3: Circular cell honeycomb arrangement 52

Plate4.4: Square cell honeycomb arrangement 52

Plate4.5: Rectangular cell honeycomb arrangement 53

LIST OF APPENDICES

	Page
APPENDIX I: Table of measured solar data for December 2005	77
APPENDIX II: Table of calculated solar parameters	78
APPENDIX III: Tables of Simulated Hourly Solar Insolation for Experimental Days	79
APPENDIX IV: Tables of experimental result	81
APPENDIX V: Drawings	89

NOMENCLATURE

Q_u Total useful heat output (W)

A_c Collector area (m^2)

F_R Collector heat removal factor

S Absorbed solar energy per unit area (W/m^2)

U_L Overall heat loss coefficient (W/m^2K)

T_i Water inlet temperature (K)

T_a Ambient temperature (K)

T_p Absorber plate temperature (K)

T_c Cover glass temperature (K)

$\dot{m}$ Mass flow rate (kg/s)

C_{pw} Specific heat capacity of water (kJ/kgK)

T_o Water outlet temperature (K)

ρ_w Density of water (kg/m^3)

hrp_c Radiative heat coefficient from plate to cover (W/m^2K)

hcp_c Convective heat coefficient from plate to cover (W/m^2K)

Nu Nusselt number

Ra Rayleigh number

g Acceleration due to gravity (m/s^2)

φ Coefficient of thermal expansion ($^oK^{-1}$)

T_m Mean air temperature

β Collector angle of tilt (^{0})

ΔT Temperature difference between the absorber and cover plate (K)

T_s Sky temperature (K)

T_m Mean temperature between the absorber plate and cover plate (K)

L Distance between the absorber and cover plate (m)

k Thermal conductivity of air (W/mK)

$\mathcal{V}$ Kinematics viscosity (m^2/s)

Pr Prandtl number

c_p Specific heat capacity of air (kJ/kgK)

μ Dynamics viscosity of air (Ns/m^2)

α Thermal diffusivity (m^2/s)

h_w Convective heat transfer coefficient of the wind (W/m^2K)

V Wind speed (m/s)

h_{rc_a} Radiative heat transfer coefficient between the absorber and cover plate (W/m^2K)

ε_c Emissivity of the cover plate

ε_c Emissivity of the absorber plate

σ Stefan Boltzmann constant (W/m^2K^4)

U_b The bottom heat loss coefficient (W/m^2K)

U_e The edge heat loss coefficient (W/m^2K)

U_t The top heat loss coefficient (W/m^2K)

K_i Thermal conductivity of the insulation at the bottom (W/mK)

L_i Thickness of the insulation at the bottom (m)

K_{ei} Thermal conductivity of the insulation at the edge (W/mK)

L_{ei} Thickness of the insulation at the edge (m)

A_p Absorber plate area (m^2)

H_b Beam solar radiation (W/m^2)

R_b The ratio of the beam radiation on an inclined surface to that on a horizontal surface

$(\tau\alpha)_b$ Absorptance –Transmittance product for the beam

H_d Diffuse solar radiation (W/m^2)

H_m Measured solar radiation (W/m^2)

H_T Total solar radiation (W/m^2)

R_d The ratio of the diffuse radiation on an inclined surface to that on a horizontal surface

$(\tau\alpha)_d$ Absorptance –Transmittance product for the beam

Ø Latitude of location (^{o})

n Number of day in a year

σ Declination angle

K_T Clearness index

H_o The extra terrestrial radiation (W/m^2)

I Instantaneous hourly solar insolation (W/m^2)

I_{sc} Solar constant (W/m^2)

ω Instantaneous hour angle

ω_s Sunset hour angle

NuC Nusselt number for collector with circular cell honeycomb

NuR Nusselt number for collector with rectangular cell honeycomb

NuS Nusselt number for collector with square cell honeycomb

NuW Nusselt number for collector without honeycomb

RaC Rayleigh number for collector with circular cell honeycomb

RaR Rayleigh number for collector with rectangular cell honeycomb

RaS Rayleigh number for collector with square cell honeycomb

RaW Rayleigh number for collector without honeycomb

h_cC Convective heat transfer coefficient for collector with circular cell honeycomb (W/m^2K)

h_cR Convective heat transfer coefficient for collector with rectangular cell honeycomb (W/m^2K)

h_cS Convective heat transfer coefficient for collector with square cell honeycomb (W/m^2K)

h_cW Convective heat transfer coefficient for collector without honeycomb (W/m^2K)

XEC Exergetic efficiency for collector with circular cell honeycomb

XER Exergetic efficiency for collector with rectangular cell honeycomb

XES Exergetic efficiency for collector with square cell honeycomb

XEW Exergetic efficiency for collector without honeycomb

TEC Thermal efficiency for collector with circular cell honeycomb

TER Thermal efficiency for collector with rectangular cell honeycomb

TES Thermal efficiency for collector with square cell honeycomb

TEW Thermal efficiency for collector without honeycomb

Q_uC Useful heat output for collector with circular cell honeycomb (W)

Q_uR Useful heat output for collector with rectangular cell honeycomb (W)

Q_uS Useful heat output for collector with square cell honeycomb (W)

Q_uW Useful heat output for collector without honeycomb (W)

r_i Ratio of hourly to daily solar insolation

a,b Instantaneous hourly radiation constant

CHAPTER ONE

INTRODUCTION

1.1 Introduction

Flat plate solar collectors are the most widely used solar collectors because of their simplicity and wide range of important potential applications. The flat plate solar collectors have been for many years the most popular device for heating water or other liquids to moderate temperatures (Rai, 2005).

Considerable effort has been made over the years to improve the efficiency and output temperatures of flat plate collectors. This effort has been made with several goals in mind. One is to store heat more efficiently for use during nights and cloudy days. The other is to increase the temperature so that tasks other than simply providing hot water are possible.

The improvement in the performance of a flat plate solar collector requires the suppression of conductive, convective and radiative heat losses from the absorber plate. The use of top glass cover prevents the loss of energy via long wave radiation as glass is opaque to it. The radiative losses from the absorber can further be reduced by the use of spectrally selective absorber coatings, Such coatings have a high absorbance of about 0.9 in the solar spectrum and a low emittance usually of the order of 0.1 in the infra-red spectrum in which the absorber radiates to the environment (Meyer et.al.1978). The air layer between the absorber plate and glass cover is a good insulator against conductive heat loss as air has a low thermal conductivity. This remains so only if the air is stagnant.

Convective heat loss through the air layer is due to the air circulation initiated within the layer when the viscous forces cannot damp out disturbances to the air layer. This condition may be brought about when the air layer is subjected to an adverse temperature gradient i.e. the

temperature of the air next to the absorber plate is higher than that next to the glass cover. In such case there will be density variation between air near the absorber plate and that near the cover glass. Thus top-heavy situation becomes unstable when the buoyancy forces (tending to cause motion) are greater than the viscous damping forces.

The Various heat losses from the absorber to the ambient are shown in figure 1.1.

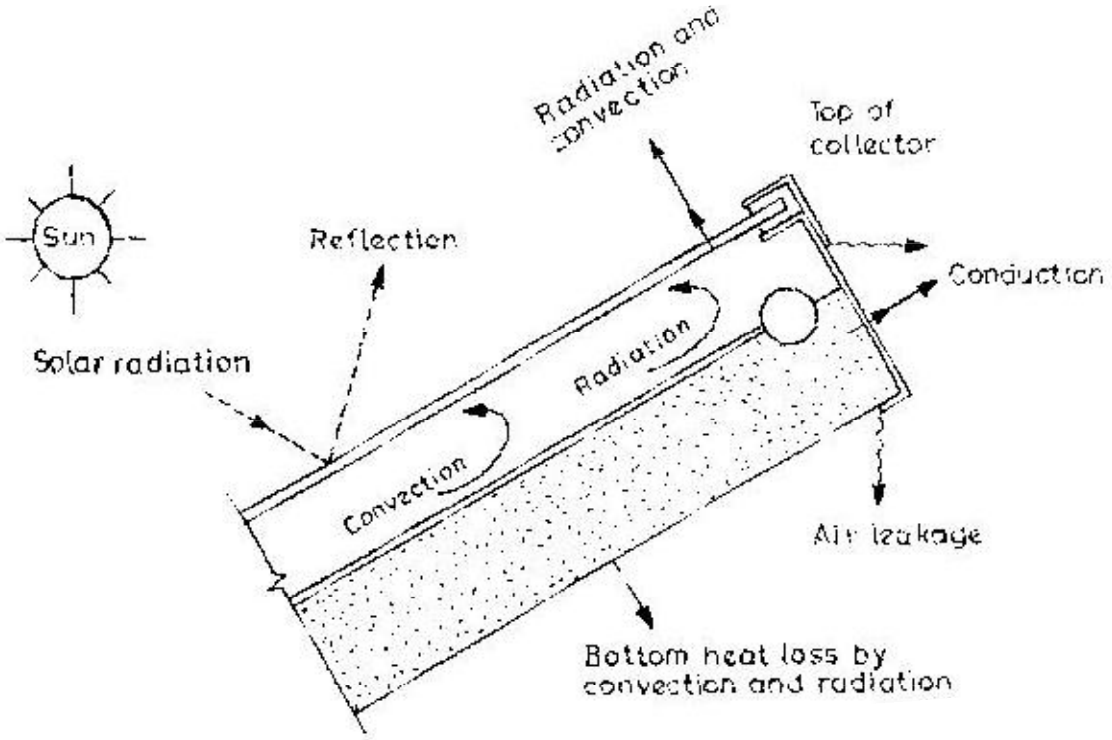


Figure1.1: Various heat losses from the absorber to the ambient (Tiwari, 2006)

Sayigh (1978) established that in a flat plate solar collector, the convective loss is about 30%. Suppressing this loss will lead to a better efficiency. There are several ways in which this can be achieved, which include the evacuated collector, the pressurized collector and the honey comb collector. The least difficult method of suppressing convection is the use of a honey comb structure.

Honeycomb solar collector is used to describe an array of cells which are essentially individual and having a small aspect ratio. Cells of honeycomb can be of various sizes and shapes such a cylindrical, square, rectangular, hexagonal etc. A schematic diagram of a square cell honeycomb is given in figure 1.2 below

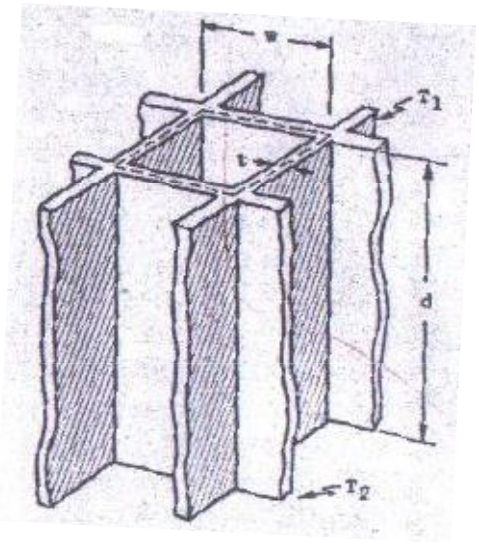


Figure1.2: Schematic diagram of a square cell honeycomb (Meinel et.al. 1976)

1.2 Statement of the Problem

Water heating constitutes about 50% of domestic heating requirement. This is mostly done by the use of electric heater or burning of fossil fuel. Due to erratic power supply in towns and cities as well as non availability in most villages of Nigeria, Fossil fuel (i.e. fuel wood, kerosene etc.) which is the most viable alternative is expensive and contribute to global warming remains the main energy source.

In Nigeria with abundant sunshine, solar energy is the most available and accessible form of energy. The acceptability of solar system has increased as an alternative to the use of fossil fuel due to the low running cost and sustainable environmental development. In order to further increase the acceptability of solar system there is need to look inward to improve on the performance of the system.

1.3 Objective of the Study

The objective of this work is to evaluate the performance of flat plate solar collectors with different honey comb geometries by comparing the rise in water temperature and collector efficiency in order to determine the most appropriate geometry for water heating.

1.4 Justification of the Study

1. Many studies on the convection suppression with the use of honeycomb have been carried out but there has not been any concerted effort to compare the efficiency of different geometries of honeycomb
2. There has been high demand of solar collectors running at high efficiency to significantly save fuel
3. Solar energy is available in abundance in Nigeria and should be tapped and used efficiently.
4. Solar water heaters are easy to operate, have long life span and are environmental friendly (i.e. do not contribute to global warming).

CHAPTER TWO

LITERATURE REVIEW

2.1 Flat Plate Solar Collectors

A flat plate solar collector is a heat exchanger capable of using solar radiation to increase the temperatures of the working fluid. It is the most common device for solar energy collection at temperatures near those required for residential use. The common arrangement of a flat plate collector is shown in the figure2.1 below.

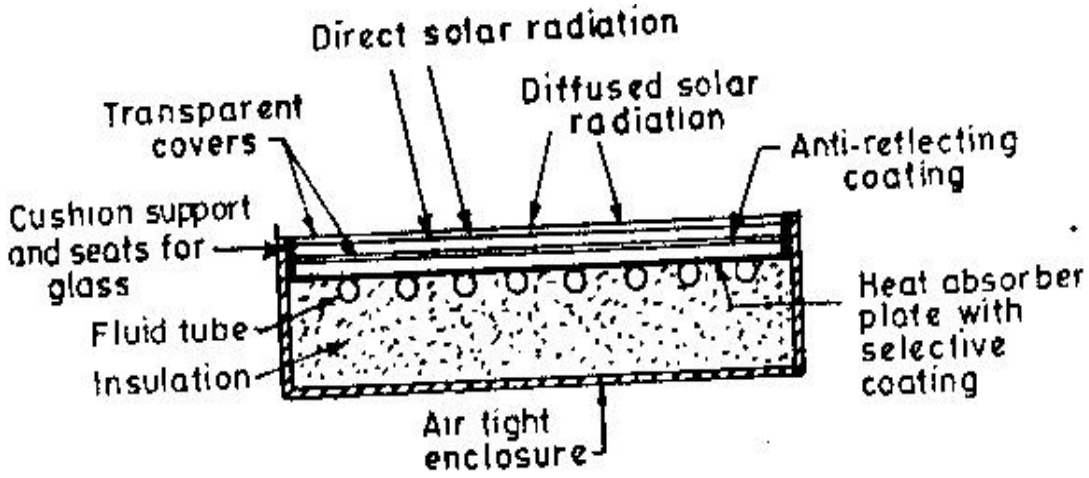


Figure2.1: The common arrangement of a flat plate solar collector (Rai, 2005)

The basic parts consist of an absorber plate, transparent or translucent cover sheets, and insulated box. The absorber is usually a sheet of high thermal conductivity metal with tubes or ducts either integral or attached. The absorber surface is painted black to maximise radiant energy absorption and in some cases to minimize radiant emission. The glazing allows sunlight to pass through to the absorber but insulate the space above the absorber so that ambient air does not blow against the absorber surface. The insulated box provides structure and sealing and reduces heat loss from the back or sides of the collector.

Flat plate collectors will absorb energy coming from all direction above the absorber (both beam and diffuse solar irradiance). Because of these characteristics, flat-plate collectors do not need to track the sun. They receive more solar energy than a similarly connected concentrating collector but have greater cosine losses. They cost less than concentrating collection because of the lack of need for a complex tracking system

Because of their potential to produce low-temperature energy for a given cost, flat plate collectors have been considered for use as pre heaters for concentrating collectors in high-temperature industrial process heat systems.

2.2 Absorber Plate

The main element of a flat plate collector is the absorber plate. It covers the full aperture area of the collector and performs the following functions.

1. Absorb the maximum possible amount of irradiance,
2. Conduct this heat into the working fluid at a minimum temperature difference
3. Lose a minimum amount of heat back to the surroundings.

2.2.1 Absorption: Solar irradiance passing through the glazing is absorbed directly by the absorber plate without intermediate reflection as in concentrating collector. Surface coatings that have a high absorptance for short wavelength (visible) light, are used on the absorber. Usually these coatings appear dull or flat indicating that they will absorb radiation coming from all directions. Either painting or plating is used and the resulting black surface will typically absorb over 95% of the incident solar radiation.

2.2.2 Fin Heat Removal: The second function of the absorber plate is to transfer the absorbed energy into the working fluid at a minimum temperature difference. This is normally done by

conducting the absorbed heat to tubes or ducts that contain the working fluid. The working fluid may either be a liquid (water) or gas (air).

The important design criterion here is to provide sufficient heat transfer surface such that the difference between the temperature of the absorber surface and the working fluid is not excessive; otherwise, the heat loss from the absorber would be high.

The absorber plate often consists of a flat sheet of metal with tubes spaced 4-5 tube diameter apart and attached to it in some fashion (Integral, brazed or press fitted). The sheet of metal absorbs most of the solar irradiance and acts as a fin to bring the absorbed heat into the fluid. The following are the important points in designing a good tube and sheet absorber.

1. The fin (absorber sheet) must be made of material with high thermal conductivity
2. Tubes should not be spaced too far apart; otherwise a higher temperature difference between the tip of the fin (midway between the tubes) and the base will result.
3. Tubes should be thin-walled and of a high-thermal conductivity material
4. The tube should be brazed or welded to the absorber sheet to minimize thermal contact resistance.
5. The tube and absorber sheet should be of similar material to prevent galvanic corrosion between them.

2.2.3 Emittance: - Because the temperature of the absorber surface is above ambient temperature, the surface re-radiates some of the heat it has absorbed back to the surroundings. This loss mechanism is a function of the emittance of the surface. Dull black paints are mostly used to enhance the absorption of sunlight (Short wavelength radiation), they also enhance the long-wavelength radiation loss from the surface. A class of coatings, mostly produced by

metallic plating processes, will produce an absorber surface that is a good absorber of short-wavelength solar irradiance but a poor emitter of long-wavelength radiant energy. These coatings are referred to as selective surfaces. Absorbers that have selective surface typically loose less heat when operating at high temperature.

2.3 Cover Sheets

The absorber is usually covered with one or more transparent or translucent cover sheets to reduce convective heat loss. In the absence of a cover sheet, heat is lost from the absorber as a result of not only forced convection caused by local wind, but also natural convective air currents created because the absorber is hotter than ambient air. The cover sheet forms a trapped air space above the absorber thereby reducing these losses. However, convective loss is not completely eliminated because a convective current is set up between the absorber and the cover sheet, transferring heat from the absorber to the cover sheet. External convection then cools the cover sheet, producing a net heat loss from the absorber.

2.3.1 Cover Sheet Material

Glass is used as the outer cover sheet on most collectors because of its superior resistance to the environment. It has transmittance of about 90% for short wave radiation and negligible transmittance for long wave radiation (Tiwari, 2006).

Plastic cover sheets are sometimes used for the second cover sheet when two sheets are required. Installation of the plastic sheet beneath the glass protects the plastic from the environment. Glass does not transmit ultraviolent radiation and thus protects the plastic, which is sensitive to this portion of the solar spectrum. Rigid sheets of acrylic or fiber glass, and reinforced polymer are

in use. Some of these plastic cover sheets have a transmittance approaching that of low iron glass. The major drawback of this scheme is the potential for overheating the plastic sheet at collector stagnation (no-flow) temperatures.

2.4 Solar Water Heating

Solar water heating is the direct use of solar energy that has been practiced most extensively in the last two decades. It is the most viable of all low-temperature solar energy applications; it will probably be the first wide use of solar energy in near future because the initial investment is small and the system is used throughout the year. The high use factor results in a higher load factor than in a solar heating system. Solar hot water heating components are now available commercially.

Solar water heater can be categorized on the basis of the means of water circulation as

I. **Passive solar water heater**

II. **Active solar water heater**

2.4.1 A passive solar water heater as shown in figure2.2 below consists of a tilted collector, with transparent cover plates, a separate, highly insulated water storage tank, and well insulated pipes connecting the two. The bottom of storage tank is higher than the top of the collector, and no auxiliary energy is required to circulate water through it. Circulation occurs through natural convection, or thermo-siphoning. When water in the collector is heated by the sun, it expands (becomes less dense) and rises up in the collector through the pipe to the top of the storage tank. This forces cooler water at the bottom of the tank out through another pipe leading to the bottom of the collector. This water, in turn, is heated and rises up into the tank. As long as the sun shines the water will quietly circulate, getting warmer. After sunset, a thermo-siphon system can reverse its flow direction and lose heat to the environment during the night. For this type of water

heater, the height of the storage tank above the top of the solar collector is an important design parameter.

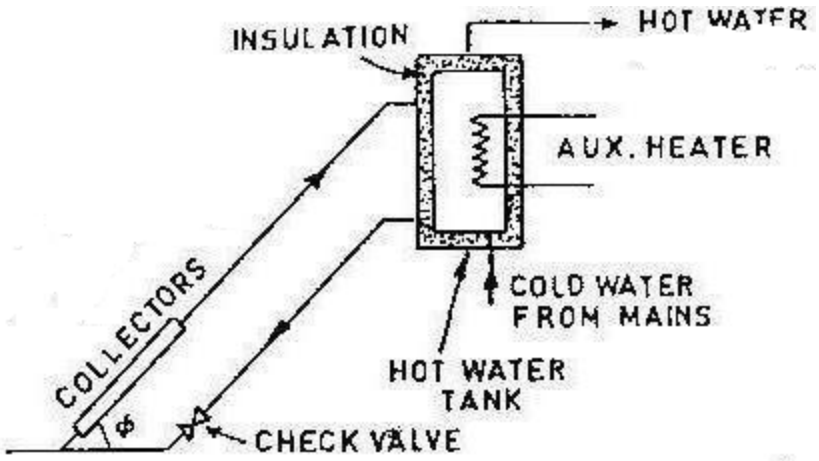


Figure2.2: Passive solar water heater (Rai, 2005)

2.4.2 An Active solar water heater: Figure2.3 below shows the schematic diagram of an active solar water heater. Here there is no requirement for location of the tank above the collector. The additional components required include a pump, motor, and a pump controller (a differential thermostat between tank and collector). A check valve is needed to prevent reverse circulation and resultant night time thermal losses from the collector.

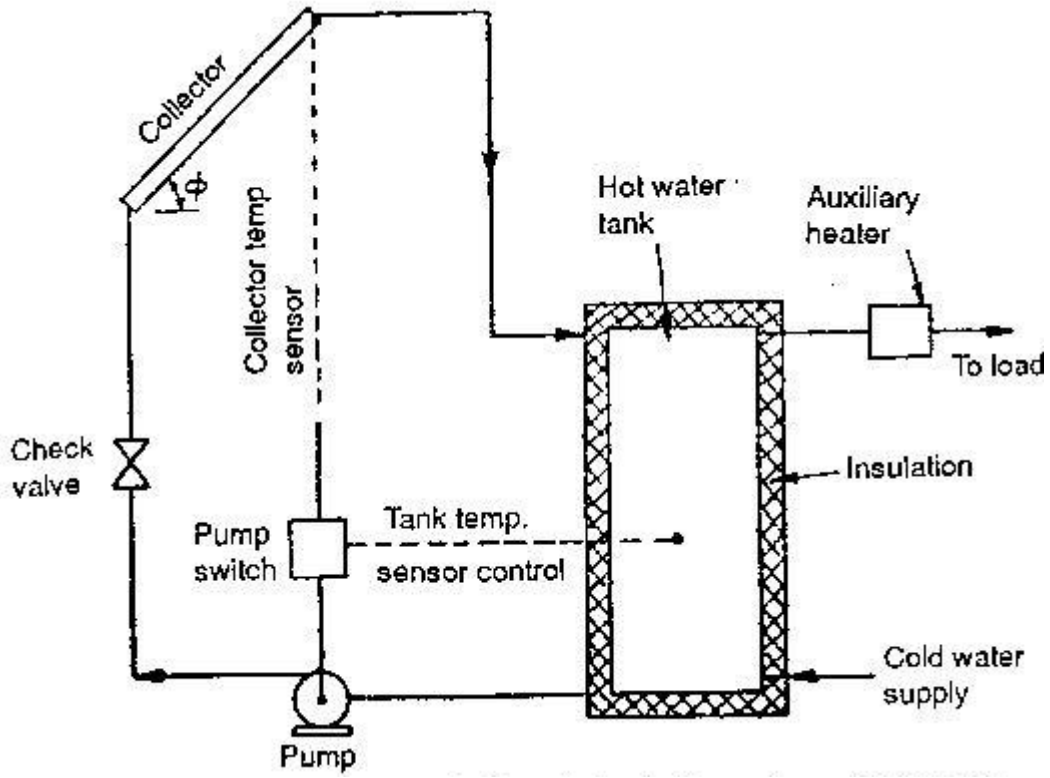


Figure 2.3 Active solar water heaters (Rai, 2005)

Solar heater can also be grouped as continuous flow or closed loop solar water heater. For a continuous flow solar water system, tap water can be used directly as shown in figure2.4 below

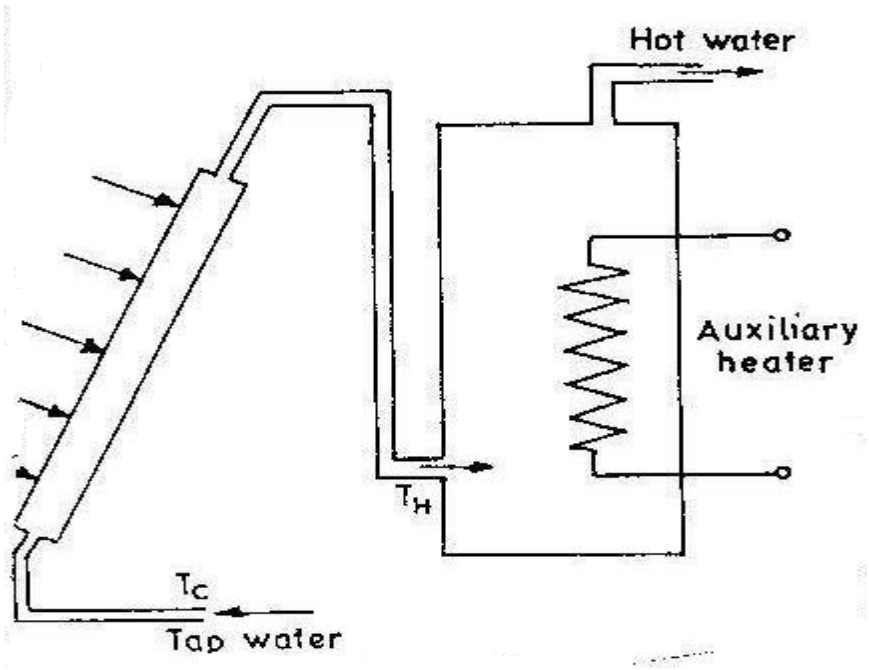


Figure2.4: continuous flow solar water heater (Rai, 2005)

While the closed loop solar water heater is similar to the thermo-siphon system described above.

2.5 Honeycomb Cell

Honey comb cells are open-ended cells whose axes are parallel to the normal vector of the plane of the glazing. They achieve high light transmittance because the cell walls are perpendicular to the plane of the glazing, and thus, any light that reflects from the cell wall continues in the forward direction. Figure 2.5 illustrate the light transmittance in a square cell honeycomb.

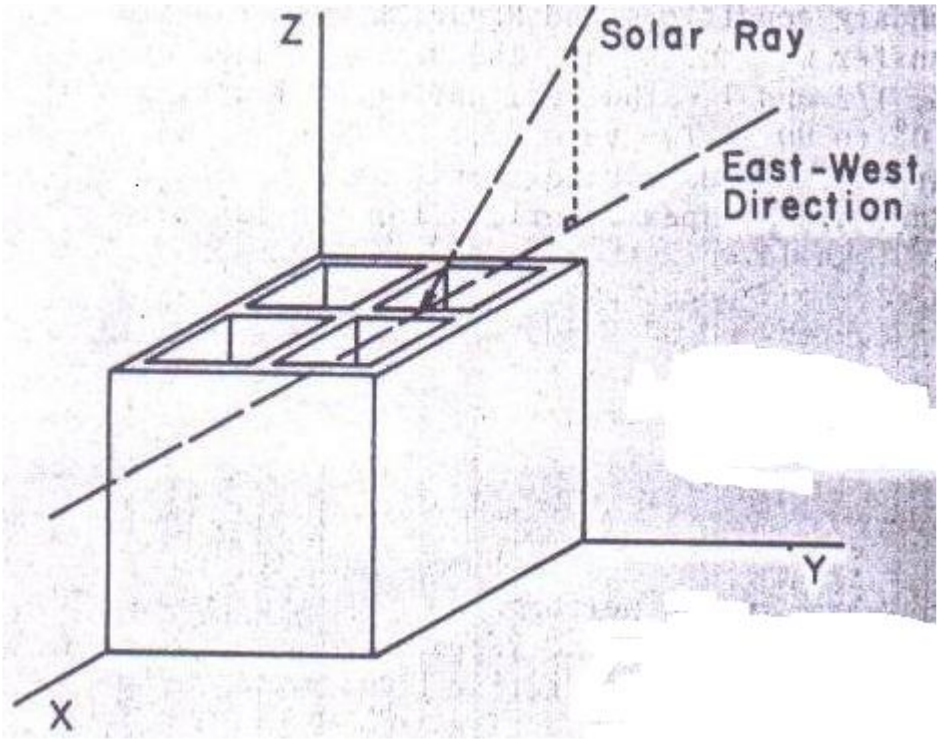


Figure2.5: Light transmittance in a square cell honeycomb (Kay et.al. 1978)

The side elevation and the plan view of a two dimensional honeycomb is given in figure2.6 below, where S is the lateral distance between the honeycomb and H is the height of the honeycomb

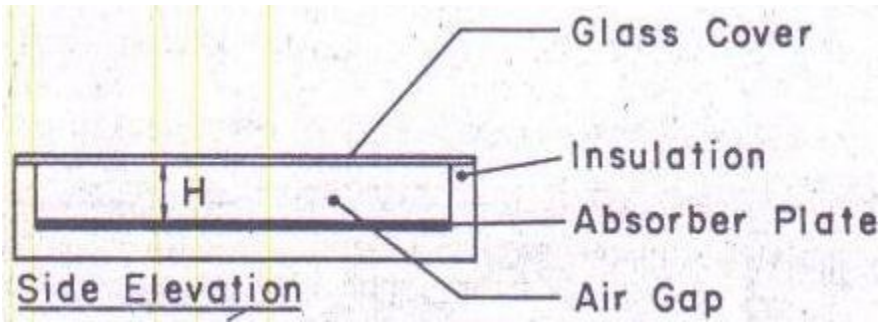


Figure 2.6a: side view of a two dimensional honeycomb (Kay et.al. 1978)

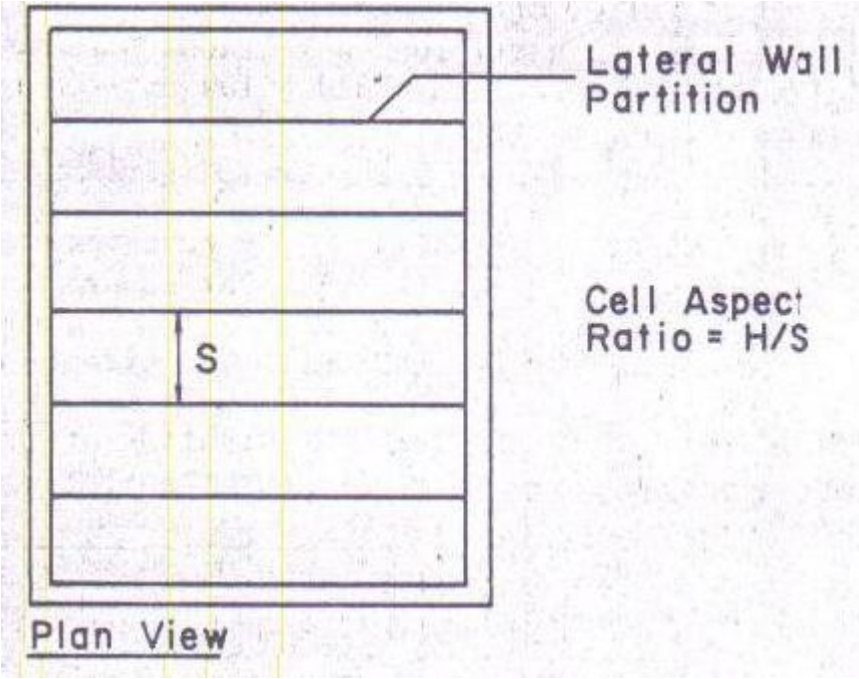


Figure 2.6b: Plan view of a two dimensional honeycomb (Kay et.al. 1978)

Honey comb cells provide insulation by suppressing both convection and radiant heat loss. They are typically made from glasses, transparent plastics such as acrylic, polycarbonate, and polypropylene etc.

It has been found that vertical convection does not begin until certain finite temperature difference between the top and bottom of the channel is exceeded (i.e. natural convection is not as soon as heat is applied but only after a minimum heating of the bottom layer as occurred). A certain minimum Rayleigh number (Ra) must be exceeded for the onset of convection

Like many other thermal insulators, honey comb insulation works by dividing an air gap into spaces that are too small to support free convection. It has been found both experimentally and theoretically that honey comb cells with hydraulic diameter on the order of 1cm (US Patent Number, 4949704) are sufficiently small to support free convection. Thus an appropriately designed honey comb transparent insulation material does a thorough job of creating a dead air layer. Using smaller cells provides little improvement in suppressing the non-radiative portion

of heat transfer but does increase the amount of material required to manufacture the honeycomb.

The suppression of convective heat is only effective for certain limit of temperature differences between the bottoms and top of the honeycomb. If the absorber temperature rose beyond a certain minimum, then the value of convective heat transfer will cause the Ra value to exceed the limit and convection will begin.

The expected variation of convective heat loss with increasing temperature difference for a honeycomb is shown in the figure2.7 below. Convection normally grows approximately linearly with temperature $T^{5/4}$ and is shown by the dashed line .when the Rayleigh number is sufficiently low, and when either the cell spacing or temperature difference is small, the convection will be fully suppressed. When the Rayleigh number reaches about 2000, the convection begins, and it rises rapidly to reach the normal convection level.

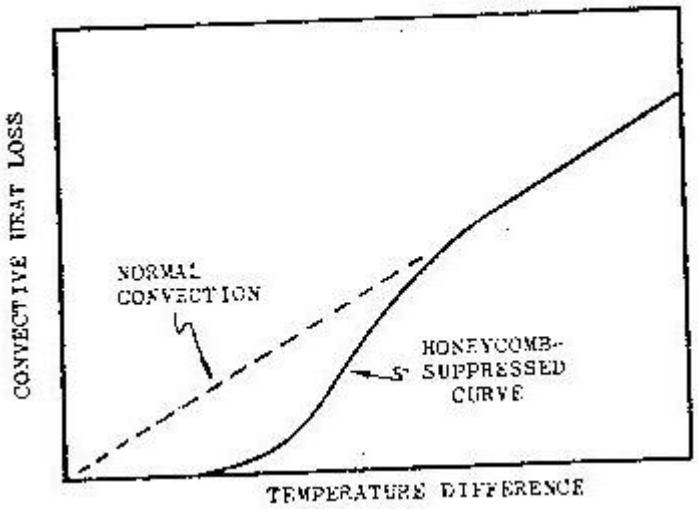


Figure2.7: Variation of convective heat loss with increasing temperature difference for a honeycomb. (Meinel et.al. 1976)

To achieve maximum insulation value; a material must suppress radiative heat transfer in addition to conduction. The rate of radiant heat transfer through a honeycomb transparent

insulation depend on the thermal-radiative emissivity of the boundary (i.e. the sheets of glass or plastic adjacent to the honey comb), the thermal-radiative emissivity of the cell wall, and the aspect ratio of the cell (i.e. as the ratio of the cell height to hydraulic diameter).

Boundary emissivity is generally a function of the glazing system which is used, and not a function of the honeycomb material itself. Thus system with high-emissivity boundary on the order of 0.9 such as glass or sheet plastic of thickness 1mm or more should be used (U.S. Patent Number, 4949704).

To improve the radiant suppression (and therefore improve the insulation value) of a typical honey comb structure which are partially transparent to thermal radiation, it is necessary to either

1. Increase the aspect ratio of the honeycomb or
2. Increase the emissivity of the cell walls for short wave radiation

To accomplish (1), it is necessary to either use a smaller cell diameter or a larger cell length (i.e. overall honeycomb thickness). But, both modification means extra material usage and cost as the material content increases with the inverse square of the cell diameter and in proportion to the honeycomb thickness (i.e. $M \alpha t/d^2$). Practical limitations may discourage greater thickness, for example finished glazing units made of such insulation sandwiched between the glass and the absorber may be too thick to work with existing framing systems. Therefore option (2), i.e. increasing wall emissivity is attractive and forms the basis for the present experiment.

It is highly desirable to use material that is inherently a strong absorber of thermal-infrared radiation. Inorganic material, such as glass or silica are highly attractive materials for making transparent honey combs, having excellent clarity and high emissivity for small thickness (a layer of glass thickness of 0.03" has an emissivity of about 0.85). However, such materials are inherently difficult to work with in typical honeycomb geometries, and this has

prevented the development of optimal glass honeycomb. Plastics despite their imperfect radiative properties are much easier to work with and thus are the material of choice for today's commercial honey comb (U.S. Patent number, 4949704).

2.6 Review of Past Work

A primary objective in designing solar collector is to reduce the heat losses. Studies of convection suppression were done by Holland (1976), Edwards (1969) Butchberg et al (1976), Meyer et al (1978) and others. In their studies, two plates were placed parallel with one plate heated and the space between the plates filled with a transparent honeycomb to suppress the onset of fluid motion. Without fluid motion, the heat transfer between the plates is by conduction and radiation. Full care must be taken in designing the structure, as an improper design can lead to an increase rather than decrease in convection losses.

Holland (1965) presented the result of a theoretical study on performance of a flat plate solar collector in which a selectively transmitting honeycomb panel is monitored between the absorbing flat plate and the outer glass cover. An analogical study of the natural convection process in such panels has shown that, under certain conditions, natural convective losses can be suppressed.

Sayigh(1978) compared various flat plates with some form of honey comb structures. He observed that at 30^0C collector tilt and the efficiency will increase with increase in aspect ratio, then it will level out at about aspect ratio equivalent to 4.He stated that with optimum tilt the suppression is better than in other cases, however the use of honeycomb suppresses convection at all positions and concluded by stating that honeycomb collectors offer high efficiency, reasonably high temperatures up to 170^0C and utilize both diffusion and direct solar radiation.

Meyer et.al (1978) used an interferometric study to determine the local and average values of the Nusselt number in a honeycomb cell with varying aspect ratios, collector angles and honeycomb angles. He showed that aspect ratios between 0.5 and 10 are undesirable to the collector designer from a pure convective loss point of view because of the expected large amount of heat lost from the top of the collector. The result also showed that collectors with honeycomb cells angle perpendicular to the gravitational field (as with $\theta=60^0$ and $Ø=60^0$) is effective in reducing losses.

Kay et.al (1978) performed experiments to validate previous numerical work on natural convection in inclined wall in finite side walls. The effect of aspect ratio, inclination angle, wall boundary conditions and Raleigh number on the heat transfer was studied. He observed that the heat transfer rate at a fixed Rayleigh number decreases as the inclination angle is increased from 0^0 and reaches a minimum at an angle in the order of 10^0 to 15^0, Significant reduction in heat transfer with the use of non-conducting lateral walls to increase the aspect ratio of the partitioned space and substantial difference in thermal conductivity is evident in glass when compared with Perspex.

Ghoneim(2005) investigated the thermal performance of solar collector equipped with square cell honeycomb material adapted from a polycarbonate material. He observed that solar collector with air gaps below and above the honey comb is found to be superior in convection suppression with bottom gap thickness crucial with respect to the heat loss coefficient. The arrangement of honey comb material with bottom gap-thickness of 3mm is the optimum as it offers the highest efficiency.

Abon-Zlyen et al (1997) presented the results of an experimental study on the effect of the thickness of air gaps in the total heat transfer across a compound honeycomb confined between two isothermal and low emissivity boundaries. It was observed that as air gap thickness

increases, coupled conductive-radiative heat-transfer is reduced while the critical Rayleigh number is also reduced and convective heat transfer increases. The decrease in the Rayleigh number is moderate and the rectangular cell compound honey comb is found to be an effective convective suppressor.

Charters et al (1982) surveys the experimental work carried out at the University of Melbourne Mechanical Engineering Department and its relationship to other experimental and theoretical research reported in literature. The experimental program involved the comparative testing of two collectors, identical except that one was fitted with a convective suppression device made of parallel glass slats placed laterally across the collector between the absorber plate and the cover glass. Testing was carried out in a laboratory situation with five convection suppression devices of different aspect ratio (i.e. 0.625/1 – 4.8/1), and the most effective of these devices was tested under a range of actual operation conditions. It was found that at high operating temperatures the convection suppression device gave rise to considerable improvement in performance. Forty percent improvement in instantaneous thermal efficiency was found for fluid temperatures of about 100^0C.

Nahar et.al.(2007) Optimized the air gap between the absorber plate and cover glazing experimentally by designing three identical collector-cum storage type solar water heaters with 25,50 and 150 mm air gaps. The heater with 50 mm air gap collects 11.64% and 7.72% more energy compared with heaters having 25mm and 150 mm air gaps respectively

2.7 Conclusion of the Review of Literature

Most of the works reviewed compare the performance of collectors with specific geometry of honeycomb with collectors without honeycomb. Since no work has been carried out to compare simultaneously the performance of different honeycomb geometries the work is justified.

CHAPTER THREE

DESIGN THEORY AND CALCULATIONS

3.1 Design Theory

Under steady state condition, the useful heat delivered by a solar collector is equal to the energy absorbed by the metal surface minus the heat losses from the surface to the surrounding (Suleiman, 2007).

This principle can be stated in the relationship (Suleiman, 2007)

$Q_u=A_cF_R(S-U_L\ (T_i-T_a))$ ---------- 1

Under steady state the useful heat delivered will be absorbed by water passing through the internal passages.

Therefore (Rajput, 1999)

$Q_u=\square.C_{pw}(T_o-T_i)$ ---------- 2

$\square=\rho AV$ ---------- 3

3.2 Evaluation of the Overall Heat Loss Coefficient (U_L)

The energy loss from the collector plate consists of radiation and convection to the cover and edges and conduction to the back insulation. The thermal analysis of a single cover flat plate solar collector showing various heat losses to the surrounding is given in figure3.1 below

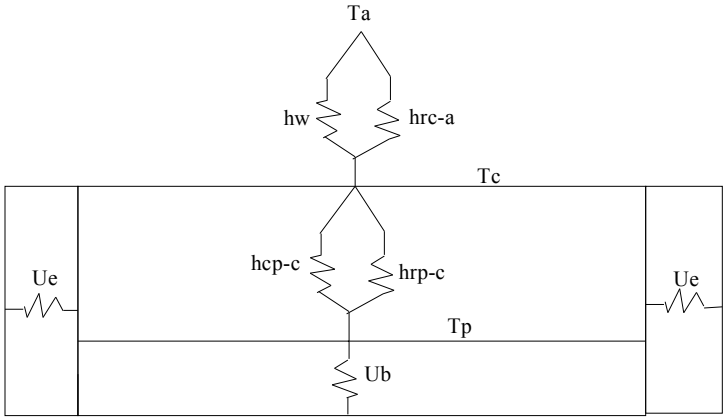


Figure 3.1: The thermal analysis of a single cover flat plate solar collector

The equivalent circuit of the thermal analysis of a single cover flat plate solar collector shown above is given in figure3.2 below.

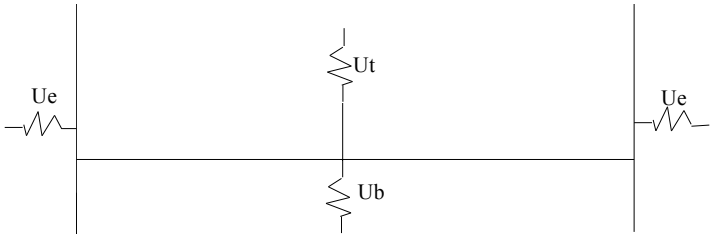


Figure3.2: The equivalent circuit of the thermal analysis of a single cover flat plate solar collector

3.2.1 Top Loss

For a single glass cover, the top loss coefficient from the collector is given by (Suleiman, 2007)

$U_t = \left(\frac{1}{hrp_c + hcp_c} + \frac{1}{hw + hrc_a}\right)^{-1}$ ---------- 4

The convective heat transfer coefficient can be obtained from the relation (Suleiman, 2007)

$h_{cp_c} = \frac{Nu.k}{L}$ ---------- 5

If the collector is sloped 0-75^o , the Nusselt number for an inclined collector is given as (Rai, 2005):

$$\text{Nu} = \left(0.069 - 0.02\left(\frac{\beta}{90}\right)\right)(Ra)^{1/3}(Pr)^{0.074} \quad \text{---------- 6}$$

$$Ra = (g\varphi\Delta TL^3)/\mathcal{V}\alpha \quad \text{---------- 7}$$

$$\varphi = \frac{1}{T_m} \quad \text{---------- 8}$$

$$T_m = \frac{T_p + T_c}{2} \quad \text{----------9}$$

$$Pr = \frac{\mu C_p}{k} \quad \text{----------10}$$

The radiative heat transfer coefficient between the plate and the cover is (Suleiman, 2007)

$$h_{rp_c} = \frac{\sigma(T_p^2 + T_c^2)(T_p + T_c)}{\frac{1}{\varepsilon_p} + \frac{1}{\varepsilon_c} - 1} \quad \text{---------- 11}$$

The convective heat transfer coefficient for the wind blowing over the collector can be obtained by(Suleiman, 2007)

$h_w = 5.7 + 3.8v$ ---------- 12

The radiative heat transfer coefficient from the cover to the sky can be obtained by (Suleiman, 2007)

$$h_{rc_a} = \varepsilon_c\sigma(T_C^2 + T_S^2)(T_C + T_S) \quad \text{---------- 13}$$

3.2.2 Bottom Loss

The bottom loss can be evaluated by (Suleiman, 2007)

$$U_b = \frac{k_i}{L_i} \quad \text{---------- 14}$$

3.2.3 Edge Loss

Assuming one dimensional sideways heat flow around the perimeter of the collector system, and the thickness of insulation at the edge and back side of the collector to be the same.

$$U_{edge} \times A_{edge} = \frac{K_{ei}}{L_{ei}} \times A_p \quad \text{---------- 15}$$

The overall heat loss coefficient can be evaluated as (Suleiman, 2007)

$$U_L = U_t + U_b + U_e \quad \text{---------- 16}$$

3.3 Heat Removal Factor

The heat removal factor is the ratio of useful energy gain of a collector to the energy gain if the whole collector surfaces were at the fluid inlet temperature and is denoted by F_R (Tiwari, 2006):

$$F_R = \frac{\dot{m}c_p(T_o - T_i)}{A_c(S - U_L(T_i - T_a))} \quad \text{---------- 17}$$

3.4 Absorbed Solar Radiation(S)

The solar energy absorbed on the surface of the sloping collector is given by(Rai, 2005):

$$S = H_b R_b (\tau\alpha)_b + H_d R_d (\tau\alpha)_d \quad \text{---------- 18}$$

(Suleiman, 2007)

$$R_b = \frac{\cos(\emptyset - \beta)\cos\sigma\cos\omega + \sin(\emptyset - \beta)\sin\sigma}{\cos\emptyset\cos\sigma\cos\omega + \sin\omega\sin\sigma} \quad \text{---------- 19}$$

σ The declination angle can be obtained from Cooper equation as

$$\sigma = 23.45 \sin\left(\frac{360(284+n)}{365}\right) \quad \text{---------- 20}$$

The ratio of the diffuse radiation on an inclined surface to that on a horizontal surface can be obtained by (Tiwari, 2006):

$$R_d = \frac{1+\cos\beta}{2} \quad \text{---------- 21}$$

3.4.1 Beam and Diffuse Solar Radiation

Collares-pereira and Rabi, 1979 express diffuse radiation as a function of clearness index

$$\frac{H_d}{H_m} =$$

$$\begin{vmatrix} 0.99 & K_T \leq 0.17 \\ 1.188 - 2.272K_T + 9.473K_T^2 - 21.865K_T^3 + 14.648K_T^4 & 0.17 < K_T < 0.75 \\ -0.54K_T + 0.632 & 0.75 < K_T < 0.8 \\ 0.2 & K_T \geq 0.8. \end{vmatrix} \text{ -}$$

---------- 22

Where

$K_T = \frac{H_m}{H_o}$ ---------- 23

Is the ratio of the measured solar radiation to the extra terrestrial radiation and is being referred to as the clearness index

The extra- terrestrial radiation is given by (Rai, 2005), the reflectance is given by:

$H_o = \frac{24\times 3600}{\pi} \times I_{sc}\left(1 + 0.033cos\left(\frac{360n}{365}\right)\right)\left(\cos\emptyset\cos\sigma\sin\omega_s + \frac{2\pi\omega_s}{360}\sin\emptyset\sin\sigma\right)$ ----------24

The sunset hour angle can be calculated from the relation (Rai, 2005):

$\omega_s = \cos^{-1}(\tan\sigma\tan\emptyset)$ ----------25

The beam solar radiation can be obtained from the total solar radiation falling on the horizontal surface (Rai, 2005):

$H_m = H_b + H_d$ ---------- 26

3.4.2 Absorptance –Transmittance Product for the Beam and Diffuse Solar Radiation

Absorptance –Transmittance product for the beam radiation is given as (Rai, 2005):

$(\tau\alpha)_b = \frac{\tau_b\alpha_b}{1-(1-\alpha_b)\rho_b}$ ---------- 27

The total transmittance through the glass cover can be evaluated from

$$\tau_b = \tau_{rb} \times \tau_{ab} \quad \text{---------- 28}$$

$$\tau_{rb} = \frac{1-\rho}{1+\rho} \quad \text{---------- 29}$$

$$\tau_{ab} = e^{\left(\frac{-kt}{\cos\theta_2}\right)} \quad \text{---------- 30}$$

For beam radiation at normal incidence (Rai, 2005), the reflectance is given by:

$$\rho = \left(\frac{n-1}{n+1}\right)^2 \quad \text{---------- 31}$$

$$n = \frac{\sin\theta_1}{\sin\theta_2} \quad \text{----------32}$$

$$(\tau\alpha)_d = \frac{\tau_d \times \alpha_d}{1-(1-\alpha_d)\rho_d} \quad \text{---------- 33}$$

The total transmittance through the glass cover for the diffuse radiation can be obtained from equation (Rai, 2005):

$$\tau_d = \tau_{rd} \times \tau_{ad} \quad \text{---------- 34}$$

$$\tau_{rd} = \frac{1-\rho_d}{1+\rho_d} \quad \text{---------- 35}$$

For an unpolarized light (Rai, 2005):

$$\rho_d = \frac{1}{2}\left(\frac{\tan^2(\theta_1-\theta_2)}{tan^2(\theta_1+\theta_2)} + \frac{sin^2(\theta_1-\theta_2)}{sin^2(\theta_1+\theta_2)}\right) \quad \text{----------36}$$

$$\tau_{ad} = e^{\left(\frac{-kt}{\cos\theta_2}\right)} \quad \text{---------- 37}$$

3.5 Collector Performance

3.5.1 Thermal Efficiency

The collector thermal efficiency is defined as the ratio of the useful heat gain over any time period to the incident solar energy over the same time period (Rai, 2005):

$$\eta_c = \frac{Q_u}{H_T \times A_c} \text{ ---------- 38}$$

3.5.2 Exergy

Exergy is the maximum useful work that can be performed by a system interacting with an environment (Akinola et.al.) The exergetic efficiency is the ratio of the useful heat output to the available work.

The key exergy parameters are heat exergy (Xen).heat anergy(Xan) and exergetic efficiency can be evaluated from the following equations(OCallaghan,1981).

Heat exergy (Xen) = $\left(\frac{T-Ta}{T}\right) I$ ----------39

Heat anergy(Xan)=$\left(\frac{T_a}{T}\right) I$----------40

Where T is the temperature of the sun and is taken as 5777K

$$\eta x = \frac{Qu}{Xen} \text{ ----------41}$$

3.6 Calculation of the Hourly Radiation

The thermal efficiency and exergetic efficiency are the index used in determining the performance characteristic of the flat plate solar collectors. In order to determine this performance characteristics the instantaneous hourly solar insolation are required. The daily solar radiation data for the test days were obtained from the meteorological department of Nigeria College of Aviation technology Zaria and were given in appendix I. the hourly solar insolation is obtained from the correlation equation given in equation (42) below.

$I = \frac{r_i x\ H_T}{3600}$----------42

$r_i = \frac{\pi}{24}(a + bcos\omega)\left(\frac{cos\omega - cos\omega_s}{sin\omega_s - \frac{\pi\omega_s}{180}cos\omega_s}\right)$ ----------43

$a = 0.409 + 0.5016\sin(\omega_s - 60)$----------44

$b = 0.6609 - 0.4767\sin(\omega_s - 60)$----------45

3.7 Honeycomb Design

Hydraulic diameter D_h is given as:

$D_h = \frac{4A}{P}$ ---------- 46

Where A is the cross sectional area of the honeycomb cell and P is the wetted perimeter of the honeycomb cell.

3.8 Design Calculations

The collector will be required to heat 1.5 Litre/hr of water to 40^o above the water inlet temperature.

INITIAL DATA	CALCULATIONS	RESULTS
c_{pw} $= \frac{4200J}{kgK}$ $\Delta T = 40^o$ AV= 1.5 Litre/hr	$\dot{m} = \rho AV$ $\dot{m} = 1000 \times \frac{1.5 \times 10^{-3}}{3600}$ $= 4.167 \times 10^{-4}\ kg/s$ From equation (2) $Q_u = \dot{m}c_{pw}(T_o - T_i)$	The useful heat that will be required to raise the temperature of water of 1.5L/hr by 40^o is 70W.

	Q_u = 4.167 X 10^{-4} X 4200 X 40 = 70W	

From equation (1)

$$Q_u = A_c F_R\left(S - U_L(T_i - T_a)\right)$$

To determine the absorbed solar radiation(S)

The design of the absorbed solar radiation will be based on the daily insolation obtained from the Nigeria meteorological department of the Nigeria college of Aviation Technology (NCAT) Zaria.

From literature and available data, the lowest solar radiation takes place in the month of December, therefore this design will be based on the month of December so that the testing can be carried out throughout the year.

Absorptance-Transmittance Product for Beam Radiation.

INITIAL DATA	CALCULATIONS	RESULTS
For plane glass with refractive index of 1.53	For beam radiation, the reflectance at normal incidence from eq 31 $\rho = \left(\frac{n-1}{n+1}\right)^2$ $\rho = \left(\frac{1.53-1}{1.53+1}\right)^2 = 0.044$ The transmittance considering the reflectance for beam radiation can be calculated from eqn 29 as	The transmittance considering the reflectance for beam radiation is 0.92

For plane glass with refractive index of 1.53 The thickness of the glass (t)=3mm The extinction constant for glass k = 0.07/cm	$\tau_{rb} = \frac{1-0.044}{1+0.044} = 0.92$ The transmittance considering the absorptance by the cover for the beam radiation from eqn 30 $\tau_{ab} = e^{\left(\frac{-kt}{\cos\theta_2}\right)}$ At normal incidence $\theta_1 = \theta_2 = 0$ $\tau_{ab} = e^{\left(\frac{-0.07\times 0.3}{\cos 0}\right)} = 0.979$ The total transmittance for the beam radiationfrom eqn 28 is $\tau_b = \tau_{rb} \times \tau_{ab} = 0.92 \times 0.979 = 0.9$	The total transmittance for the beam radiation is 0.9
The surface of the absorber will be painted with black paint. the absortance for black paint from literature is between 0.95 and 0.98. Take the absorptance =0.95	the absorptance-transmittance product for the beam radiation is $(\tau\alpha)_b = \frac{0.9 \times 0.95}{1-(1-0.95)0.044} = 0.86$	the absorptance-transmittance product for the beam radiation is 0.86

Absorptance-Transmittance Product for Diffuse Radiation

INITIAL DATA	CALCULATIONS	RESULTS
The diffuse radiation can be estimated by assuming the incident angle to be 60^o $\theta = 60^o$	$n = \frac{\sin\theta_1}{\sin\theta_2}$ θ_2 $= \sin^{-1}\left(\frac{\sin\theta_1}{n}\right)$ n $= 1.53$ $\theta_2 = \sin^{-1}\left(\frac{\sin 60}{1.53}\right) = 34.47^o$ The diffuse reflectance can be obtained from eqn 36 $\rho_d = \frac{1}{2}\left(\frac{\tan^2(\theta_1 - \theta_2)}{tan^2(\theta_1 + \theta_2)} + \frac{sin^2(\theta_1 - \theta_2)}{sin^2(\theta_1 + \theta_2)}\right)$ $\rho_d = \frac{1}{2}\left(\frac{\tan^2(60 - 34.47)}{tan^2(60 + 34.47)} + \frac{sin^2(60 - 34.47)}{sin^2(60 + 34.47)}\right)$ $= 0.094$ The transmittance considering reflectance for the diffuse radiation from eqn 33	The diffuse reflectance is 0.094 The transmittance considering reflectance for the diffuse

	$\tau_{rd} = \frac{1 - 0.094}{1 + 0.094} = 0.828$ The transmittance considering absorptance of the cover for the diffuse radiation can be obtained from eqn 37 $\tau_{ad} = e^{\left(\frac{-kt}{\cos\theta_2}\right)}$ $\tau_{ad} = e^{\left(\frac{-0.07 \times 0.3}{\cos 34.47}\right)} = 0.975$ The total transmittance for the diffuse radiation from eqn $\tau_d = \tau_{rd} \times \tau_{ad}$ $\tau_d = 0.828 \times 0.975 = 0.81$ The transmittance absorptance product for the diffuse radiation is $(\tau\alpha)_d = \frac{0.81 \times 0.95}{1 - (1 - 0.95)0.094} = 0.77$	radiation=0.828 The total transmittance for the diffuse radiation is 0.81 The transmittance absorptance product for the diffuse radiation is 0.77

Calculation of the Beam and Diffuse Radiation

The beam and diffuse radiation for each day in December will be calculated.

INITIAL DATA	CALCULATIONS	RESULTS
For December 1 the measured solar radiation on a horizontal surface is 18.8MJ/m^2	The clearness index from eqn 23 is $K_T = \frac{H_m}{H_o}$ For December 1 n=335 The declination from eqn20 $\delta = 23.45 \sin\left(\frac{360 \times (284 + 335)}{365}\right)$ $= -22.11^o$ The sunset hour angle from eqn25 $w_s = \cos^{-1}(-\tan \emptyset \tan \delta)$ The latitude of zaria is 11^oN Therefore $\emptyset = 11^o N$ $w_s = \cos^{-1}(-\tan 11 \tan(-22.11)) = 85.47$ The solar constant is I_{sc} =1367W/m^2 The extraterrestrial radiation from eqn 24 is	The declination -22.11^o The sunset hour angle is 85.47

	H_o $= \frac{24 \times 3600}{\pi} \times 1367$ $\times \left(1 + 0.033 \cos\left(\frac{360 \times 335}{365}\right)\right)$ $\times \left(\cos 11 \cos(-22.11) \sin 85.47\right.$ $\left. + \frac{2\pi \times 85.47}{360} \times \sin 11 \sin(-22.11)\right)$ $= 30.84 MJ/m^2$ The clearness index for December 1 $K_T = \frac{H_m}{H_o} = \frac{18.8}{30.84} = 0.6096$ K_T falls between 0.17 and 0.75 Using colleres-pereira and Rabi equation from eqn 22 $\frac{H_d}{H_m} = 1.188 - 2.272K_T + 9.473K_T^2 - 21.865K_T^3 + 14.648K_T^4$ $\frac{H_d}{H_m} = 1.188 - 2.272(0.6096) + 9.473(0.6096)^2 - 21.865(0.6096)^3 + 14.648(0.6096)^4 = 0.3929$ But $H_m = 18.8 MJ/m^2$	The extraterrestrial radiation is$30.84 MJ/m^2$ The clearness index for December 1 is 0.6096

	$H_m(Watt/m^2) = \frac{H_m(J/m^2)}{sunshine\ hour \times 3600}$ For December 1 the sunshine hour in Zaria is 10.4 $H_m(Watt/m^2) = \frac{18.8 \times 10^6}{10.4 \times 3600}$ $= 502.1W/m^2$ The diffuse solar radiation $H_d = 0.3929 \times H_m = 0.3929 \times 502.1$ $= 197.3W/m^2$ The beam solar radiation from eqn 26 $H_b = H_m - H_d = 502.1 - 197.3$ $= 304.8\,W/m^2$	the measured solar radiation in W/m^2 is$502.1W/m^2$ The diffuse solar radiation for December 1 is$197.3W/m^2$ The beam solar radiation for December 1is $304.8\,W/m^2$

Calculation of the Ratio of Beam and Diffuse Solar Radiation on an Inclined Surface to that on Horizontal Surface

INITIAL DATA	CALCULATIONS	RESULTS
The angle of tilt of the collector is taken as the angle of latitude. Therefore $\beta = \varphi = 11^{o}$	The ratio of the diffuse solar radiation on an inclined surface to that on the horizontal surface is calculated from eqn 21 $$R_d = \frac{1 + \cos\beta}{2}$$ $$R_d = \frac{1 + \cos 11}{2} = 0.9908$$ The ratio of the beam radiation on an inclined surface to that on horizontal surface from eqn 19 $$R_b = \frac{\cos(11-11)\cos(-22.11)\cos 0 + \sin(11-11)\sin}{\cos 11\cos(-22.11)\cos 0 + \sin 11\sin(-22.1}$$ $= 1.106$ The absorbed solar radiation for December 1from eqn 16 $$S = H_b R_b(\tau\alpha)_b + H_d R_d(\tau\alpha)_d$$ $$= 304.8 \times 1.106 \times 0.86 + 197.3 \times 0.9908 \times 0.77 = 440.44\ W/m^2$$	The ratio of the diffuse solar radiation on an inclined surface to that on the horizontal surface is 0.9908 The absorbed solar radiation for December 1 is $440.44\ W/m^2$

The declination angle ,sunshine hour angle, extra terrestrial radiation (H_o),clearness index beam radiation diffuse radiation and absorbed solar radiation for other days in December were calculated using the Engineering equation solver(EES)and the result tabulated as given in table 1 in appendix II.

From appendix I average absorbed solar radiation

$$= \frac{Total\ absorbed\ solar\ radiation}{number\ of\ days} = \frac{12864.2}{31} = 414.97\,W/m^2$$

From equation 1

$$Q_u = A_c F_R\left(S - U_L(T_i - T_a)\right)$$

If the water inlet temperature is at ambient temperature i.e. T_i=T_a

Then

$$Q_u = A_c F_R S$$

Assume the heat removal factor to be 0.7

$$F_R = 0.7$$

$$Q_u = 0.7 A_c S$$

$$Q_u\ is\ the\ heat\ required\ to\ raise\ the\ temperature\ of\ \frac{1.5l}{hr}\ of\ water\ by\ 40^o\ above$$

the $water\ inlet\ temperature$=70W

$$A_c = \frac{Q_u}{0.7S} = \frac{70}{414.97X0.7} = 0.241m^2$$

For a square collector

$$A_c = L^2$$

$$L^2 = 0.241$$

$$L = \sqrt{0.241} = 0.4909m = 49.09cm$$

Therefore, the length of the collector is taken as 50cm and the area of the collector will be

$L^2 = 0.5 \text{ X } 0.5 = 0.25 \text{ m}^2$

Thickness of Back Insulation

It is recommended that back insulation should be equivalent to at least 50mm of mineral wool (Tiwari, 2006). But fiber glass is commercially available and has lower thermal conductivity.

The equivalent thickness of the fiberglass can be obtained from the equation below.

$$\frac{K_1}{x_1} = \frac{K_2}{x_2}$$

The thermal conductivity of mineral wool is 0.04 W/mk

The thermal conductivity of fibre glass is 0.03 W/mk

The thickness of mineral wool is 50mm

$$x_{fibre\ glass} = \frac{K_{fibre\ glass} x_{mineral\ wool}}{K_{mineral\ wool}}$$

$$x_{fibre\ glass} = \frac{0.03 \times 50}{0.04} = 37.5mm$$

Therefore the design thickness of the back insulation will be 40mm.

Tube Spacing

Tube spacing is an important parameter in the design of a flat plate solar collector. The optimum spacing will give lower cost and highest fin efficiency.

Bala (1980) state that for nominal pipe diameter of 12.7mm and plate thickness of 0.794mm the optimum pipe spacing is 150mm.

For a collector width of 500mm

The number of riser = $\frac{500}{150} = 3.33$

Therefore the number of riser = 4

The required pipe spacing = $\frac{500}{4}$ = $125mm$

Honeycomb Design

From literature the hydraulic diameter of 1 cm is enough to suppress convection. Therefore the hydraulic diameter of 1 cm is chosen.

INITIAL DATA	CALCULATIONS	RESULTS
D_h = 1cm	FOR CIRCULAR CELL HONEYCOMB $A = \frac{\pi D^2}{4}$, $P = \pi D$ $D_h = \frac{4A}{P} = \frac{4 \times \frac{\pi D^2}{4}}{\pi D}$ $= \frac{\pi D^2}{\pi D} = D$ Therefore the hydraulic diameter is the same as the same as the diameter of the cell in a circular cell honeycomb. D_h = D= 1cm	the diameter of the circular honeycomb is 1cm
D_h = 1cm	FOR SQUARE CELL HONEYCOMB $A = L^2$, $P = 4L$ $D_h = \frac{4A}{P} = \frac{4L^2}{4L} = L$	D_h = L = 1 cm Therefore 1cm X 1cm will be used in square cell honeycomb

	Therefore the hydraulic diameter is the same as the same as the length of the cell in a square cell honeycomb.	
D_h = 1cm	FOR RECTANGULAR CELL HONEYCOMB $A = L \times B$, $P = 2(L + B)$ $if \quad B = \frac{L}{2}$ $A = L \times \frac{L}{2} = \frac{L^2}{2}$, $P = 2\left(L + \frac{L}{2}\right) = 3L$ $D_h = \frac{4 \times \frac{L^2}{2}}{3L} = \frac{2L}{3}$ $L = \frac{3D_h}{2}$, $B = \frac{3D_h}{4}$ Where L is the length of the cell and B is the breadth of the cell $L = \frac{3D_h}{2} = \frac{3 \times 1}{2} = 1.5cm$	Therefore the length of

	$B = \frac{3D_h}{4} = \frac{3 \times 1}{4}$ $= 0.75cm$	1.5cm and breadth of 0.75cm will be used in rectangular cell honeycomb.

Simulation of the Hourly Radiation

For day1 of the experiment the measured solar radiation is 19.4MJ/m^2

Day1 of the experiment was may1 which is 121 day of the year

INITIAL DATA	CALCULATIONS	RESULTS
H_m= 19.4MJ/m^2 N=121 A_c=0.25 m^2	The total solar radiation that falls on the collector on may 1 $H_T = H_m \times A_c = 19.4 \times 10^6 \times 0.25 = 4.85MJ$ The declination angle for May1 from eqn20 $\delta = 23.45 \sin\left(\frac{360 \times (284 + 121)}{365}\right) = 14.9^o$ The sunset hour angle from eqn25 $\omega_s = \cos^{-1}(-\tan \emptyset \tan \delta)$ The latitude of zaria is 11^oN Therefore $\emptyset = 11^o N$ $\omega_s = \cos^{-1}(-\tan 11 \tan(14.9)) = 92.96$ The hourly solar insolation constant for May1 can be obtained from equations(44&45)	The declination angle for May1 $\delta = 14.9$ The sunset hour angle

	$a = 0.409 + 0.5016\sin(92.96 - 60) = 0.6819$ $b = 0.6609 - 0.4767\sin(92.96 - 60) = 0.4015$ For 6am the hour angle $\omega = -90$ ri $= \frac{\pi}{24}(0.6819 + 0.4015\cos(-90))\, x \left(\frac{\cos(-90) - \cos(92.96)}{\sin(92.96) - \frac{\pi x 92.96 x cos(92.96}{180}} \right.$ $= 0.004265$ The simulated solar insolation for 6am on May1 from eqn42 $I = \frac{0.004265x4.85x10^6}{3600} = 5.746W$	for May1 $w_s = 92.96$ The simulated solar insolation for 6am on May1 is $5.746W$

The simulated solar insolation for other time of day1 and other experimental days were obtained using EES equation solver and presented in AppendixIII

CHAPTER FOUR

CONSTRUCTION, TESTING AND RESULTS

4.1 Introduction

The construction of the designed flat plate solar water heater is simple and can be carried out by local fabricators. The materials used were sourced locally based on availability, cost and effectiveness.

- The absorber plate was made of mild steel because of its relative cheapness
- The honeycombs were structured from glass because of its high light transmissivity and can withstand temperature above 150^{o}C which is more than the working range for flat plate solar water heater.
- The frame was made of plywood because of low thermal conductivity
- Fibre glass was used to further reduce the heat losses from the back side of the collector

4.2 Construction Processes

Four similar flat pate collectors were constructed as described below. Since the construction is repetitive in nature the construction process for one of the collector was given in the table below

S/N	COMPONENT	MATERIAL	PROCESS DESCRIPTION	EQUIPMENT USED
1	Wooden frame	19mm ply wood	Marking and cutting of a) Collector base of 538mm X 538mm b) Four sides of the collector of two(2) nos of 90mmX538mm and	Hacksaw, pencil, measuring tape, ruler

			two(2) nos of 90mm X 500mm Joining of the base and the four sides together	
2	Wedge	Planck	Marking and cutting of two (2) nos of a right angle triangle wedge support of base 490mm and height 95mm	Hacksaw, pencil, measuring tape, ruler
3	Cover glass guide	Planck	Marking and cutting of angular cover guide of a) two(2) nos of lenght538mm b) two(2) nos of length 500mm	Hacksaw, pencil, measuring tape, ruler
4	Absorber plate	1mm thickness Mild steel	The absorber plate is obtained by marking and cutting to square dimension of 500mmX500mm. 1/2" Galvanized iron pipe is marked and cut to a) two(2) header of length 600mm each b) four (4) risers of length 475mm	Hacksaw, scriber, metal rule, measuring tape, arc welding machine, electrode

			the pipe was arranged and welded to one side of the absorber plate using the arc welding techniques as shown in drawing no 10 while the other side was painted black to aid the absorption of solar radiation	
5	Cover glass	2mm plane glass	Marking and cutting of cover glass of 520mm X 520mm	Marker ,metal rule, measuring tape and point glass cutter

6	Square cell honeycomb	2mm plane glass	Each row of a Square cell honeycomb was constructed by cutting of i) 1 rectangular strip of 50mmX500mm ii) 42 rectangular strip	Marker ,metal rule, measuring tape, point glass cutter and super glue

			of 50mm X 10mm. iii) joining the two strips by placing the smaller strip at interval of 10mm on the bigger strip using super glue as adhesive	
7	Rectangular cell honeycomb	2mm plane glass	Each row of a Rectangular cell honeycomb was constructed by cutting of i) 1 rectangular strip of 50mmX500mm ii) 30 rectangular strip of 50mm X 15mm iii) joining the two strips by placing the smaller strip at interval of 8mm on the bigger strip using	Marker ,metal rule, measuring tape, point glass cutter and super glue

			super glue as adhesive	
8	Circular cell honeycomb	Capillary tube of 10mm internal diameter	The circular cell honeycomb was constructed by cutting the capillary tube to a length of 50mm each to obtain about 1600 pieces which was arranged in form of bundles within the air gap of the collector	Marker , measuring tape, blade glass cutter

4.3 Assembly of Component Parts

The assembly of all the components part produced is necessary to carry out the experimental set-up.

4.3.1 Flat Plate Solar Collector

The assembly of flat plate solar collector involves

- the joining of the frame
- Filling of the fibre glass
- Positioning of the absorber plate and the glass cover
- Fitting of the glass guide as shown in drawing no
- This processes is repeated for the three other collectors

4.3.2 Square Cell Honeycomb

To form the square cell honey comb structure as shown in drawing no 7each of the row of glass strip formed as describe in process no was arranged end to end to occupy the entire air gap within the collector

4.3.3 Rectangular Cell Honeycomb

To form the rectangular cell honey comb structure as shown in drawing no 8 each of the row of glass strip formed as describe in process no was arranged end to end to occupy the entire air gap within the collector

4.3.4 Circular Cell Honeycomb

The over 1600 pieces of cylindrical glass cut was arranged and closely packed in form of bundles to occupy the entire air gap as shown in drawing no 6

4.3.5 Water Supply System

The water supply system includes a cylindrical tank with a stand of 1m which is available in the Department of Mechanical Engineering Ahmadu Bello University Zaria.

The tank was connected to each of the solar water heater with 12.7mm PVC pipe with a valve at the entry of each collector. The outlet of the tank was also fixed with a valve to close the water outlet of the tank .the connection was made in parallel such the water inlet condition to each of the collector is similar.

4.4 Description of the Experimental Set-up

The experimental set up consist of four similar designed and constructed flat plate solar collector arranged in series as shown in figure4.1 below.

Water tank is placed at a height of 1m which is enough to support continuous free flow of water through each of the collector. Each flat plate solar collector consist of an absorber plate of 50cm x 50cm made of mild steel coated with black paint to aid its absorption and galvanized pipe arrangement welded to the backside of the absorber plate to form an integral part. The frame is made of 19mm plywood because of its low thermal conductivity. The heat loss through the back side was reduced by the use of 40mm thickness fiber glass as the insulator. Three of the collectors were sandwiched with circular, square and rectangular cell honeycomb respectively of 10mm hydraulic diameter structured from glass, while the fourth was without honeycomb (i.e. used as the control experiment).the collector was covered with glass of 3mm thickness and tilted at 11^{o} which is the latitude of Zaria. Holes were drilled at the inlet and outlet of the header pipe such that the water inlet and outlet temperature can be monitored by the use of mercury in glass thermometer .The experimental set-up is shown in plate 4.1 and 4.2 while the circular, square and rectangular cell honeycomb arrangement are shown in plate 4.3,4.4and 4.5 respectively

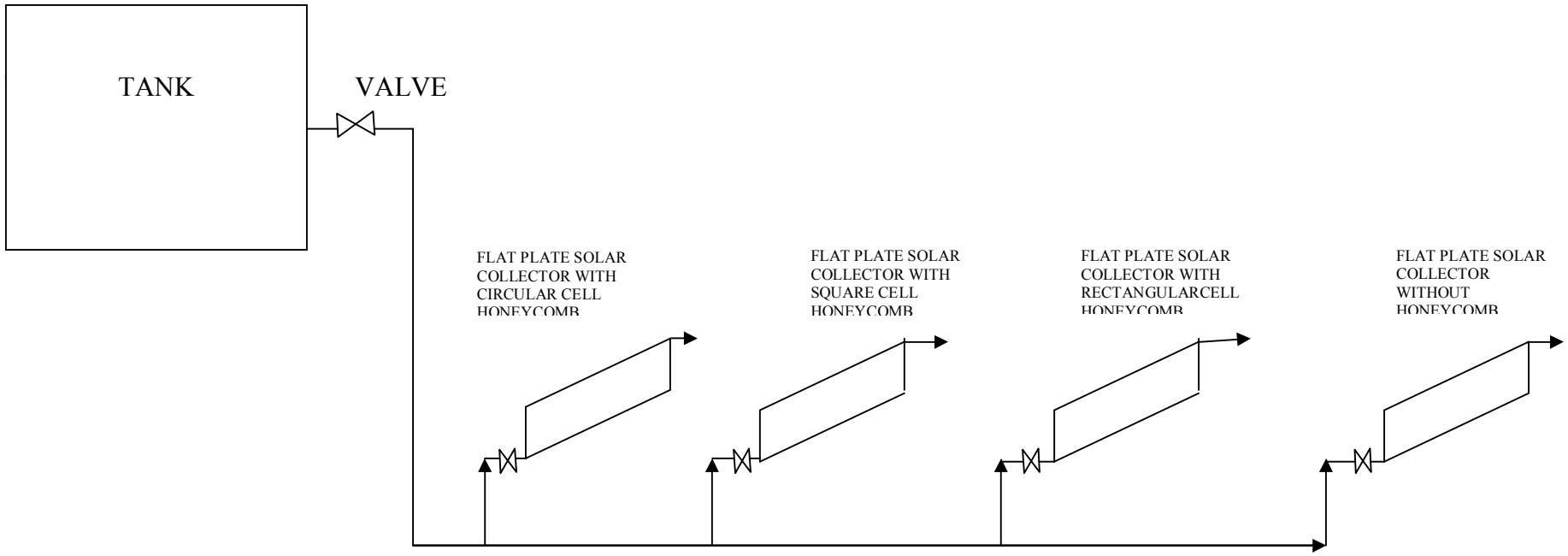


Figure4.1: FLOW DIAGRAM OF THE EXPERIMENTAL SET-UP



Plate 4.1: Front view of the experimental set-up



Plate 4.2: Side view of the experimental set-up



Plate4.3: Circular cell honeycomb arrangement

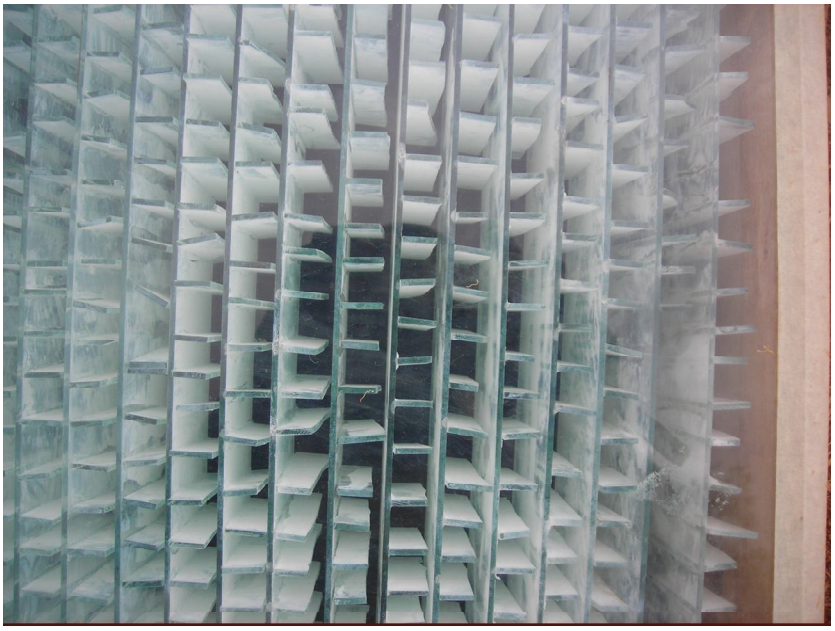


Plate4.4: Square cell honeycomb arrangement

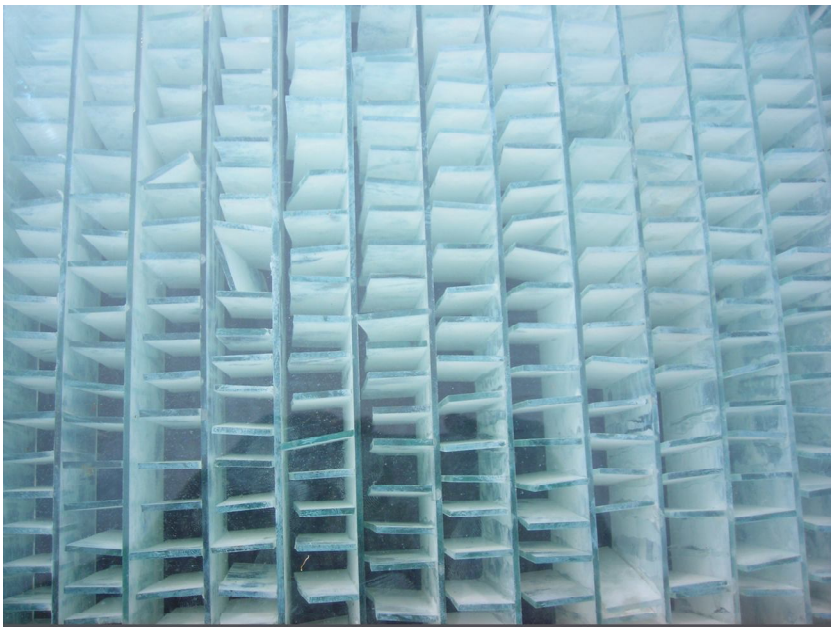


Plate4.5: Rectangular cell honeycomb arrangement

4.5 Experimentation

A comparative study of different honeycomb geometries for the suppression of convective heat transfer in flat plate solar collector was carried out. The honeycombs studied were the circular, rectangular and square cell geometry. Four similar flat plate solar collectors were designed, constructed and experiment carried out in the Department of Mechanical Engineering Ahmadu Bello university Zaria between 1st and 7th of May 2009.

Water was allowed to flow through each of the collector from the tank in a continuous flow process. This was achieved by connecting a continuous flow tap water to the top of the tank via a hose. The water inlet and outlet temperatures as well as the ambient temperature were measured using mercury in glass thermometer while the absorber plate and cover plate temperatures were measured using thermocouples on hourly basis between 0800hr and 1600hr local time and the result presented as shown from table 1 to table 16 in appendix II.

4.6 Results and Discussion

The Rayleigh number and Nusselt number were calculated using equations (7) and (6) respectively from where the convective heat transfer coefficient was calculated using equation (5). The hourly useful heat output and the available energy (exergy) of the collector were calculated using equations (2) and (39) respectively from where the thermal efficiency and exergetic efficiency were obtained using equations (38) and (41) respectively and the results were presented on table1 to table 14 in appendix IV.

From the tables, the relationship between the Rayleigh number, Nusselt number, convective heat transfer coefficient, useful heat output, thermal efficiency and exergetic efficiency were plotted against the local time for day 1 to day4 as shown in figure 4.2 through figure 4.25 below.

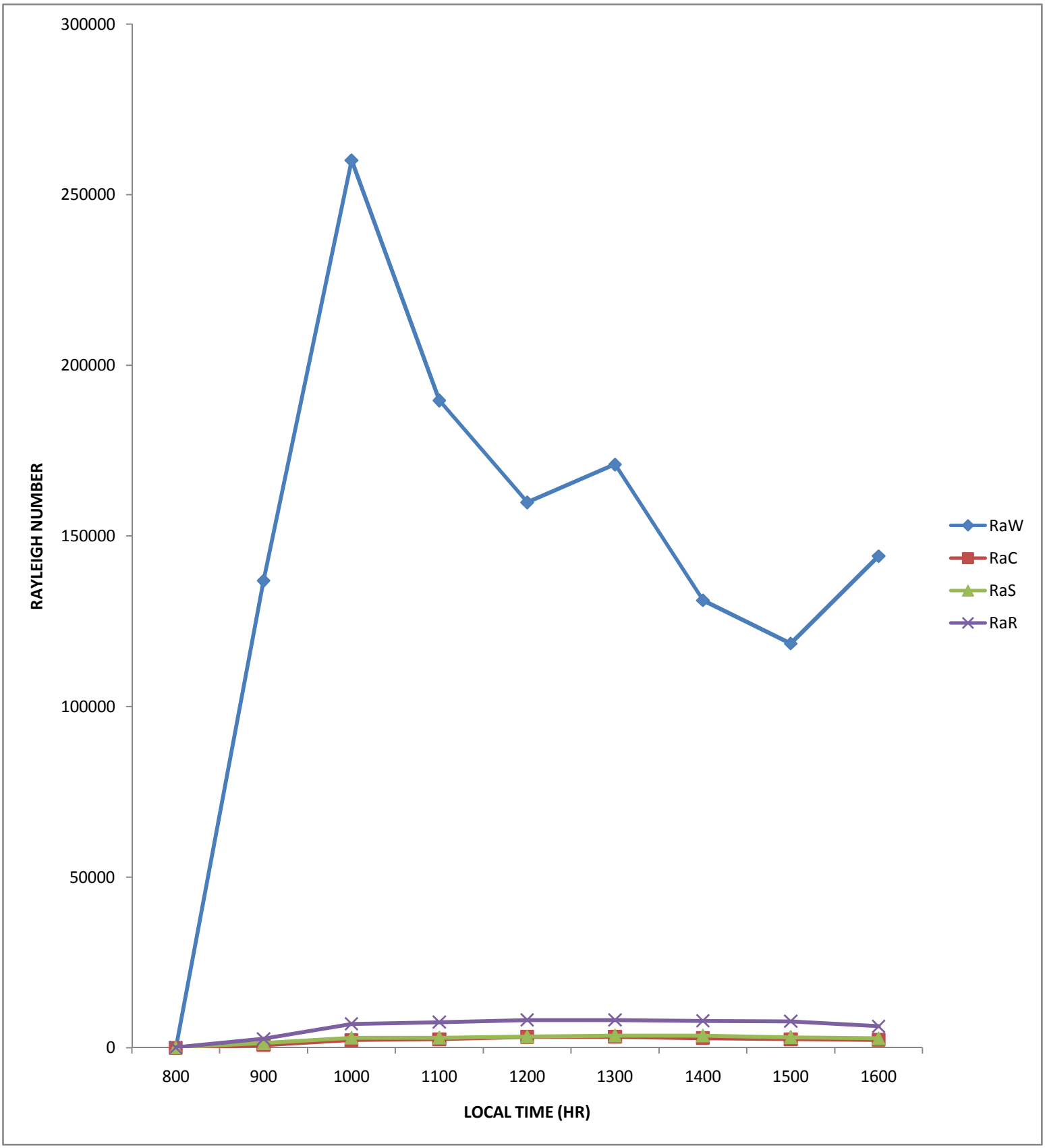


Fig 4.2: Graph of the Rayleigh number against the local time for day1

For day1, Figure4.2 shows that the Rayleigh number for the collector without the honeycomb was far more than those of the collectors with honey comb which justified that the collector without honey has higher Nusselt number and convective heat transfer coefficient than those with honeycomb as shown in figure 4.3 and figure 4.4 respectively.

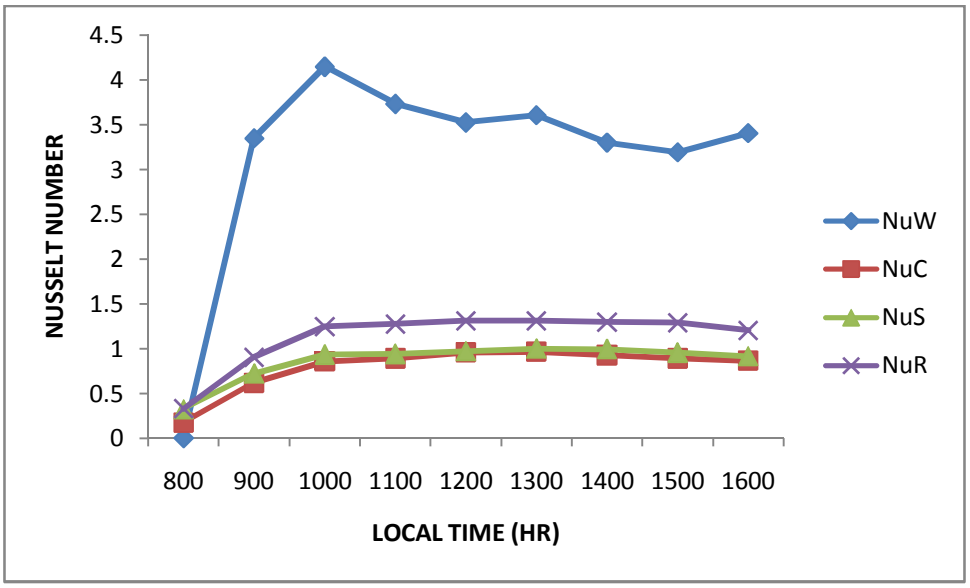


Fig 4.3: Graph of the Nusselt number against the local time for day1

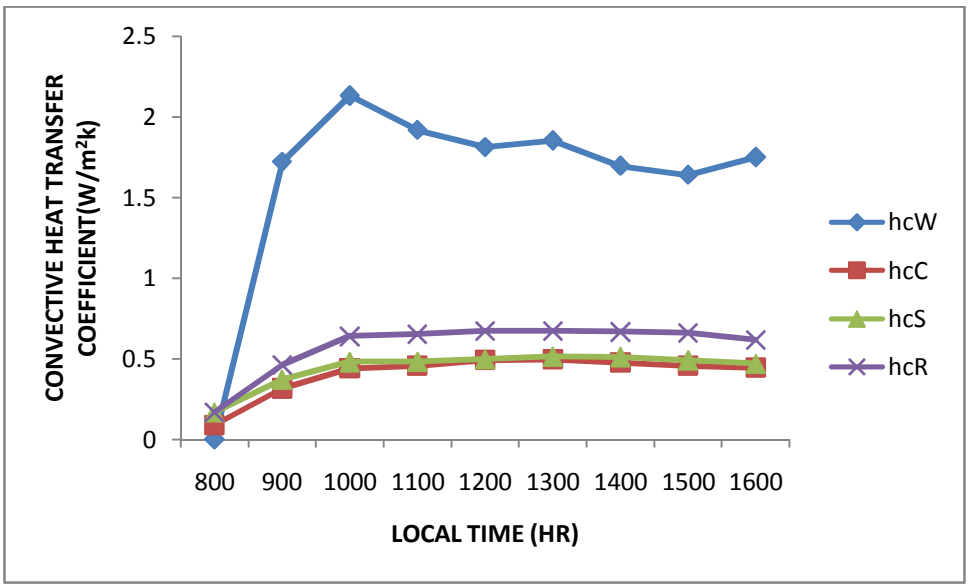


Fig 4.4: Graph of the Convective heat transfer coefficient against the local time for day1

The collector with circular cell honeycomb has the least Rayleigh number, Nusselt number, and convective heat transfer coefficient follow by the collector with square cell and rectangular cell honey comb respectively .This means that the rate of heat losses from the absorber plate is highest in the collector without honey comb followed by that with rectangular, square and circular cell honey comb respectively.

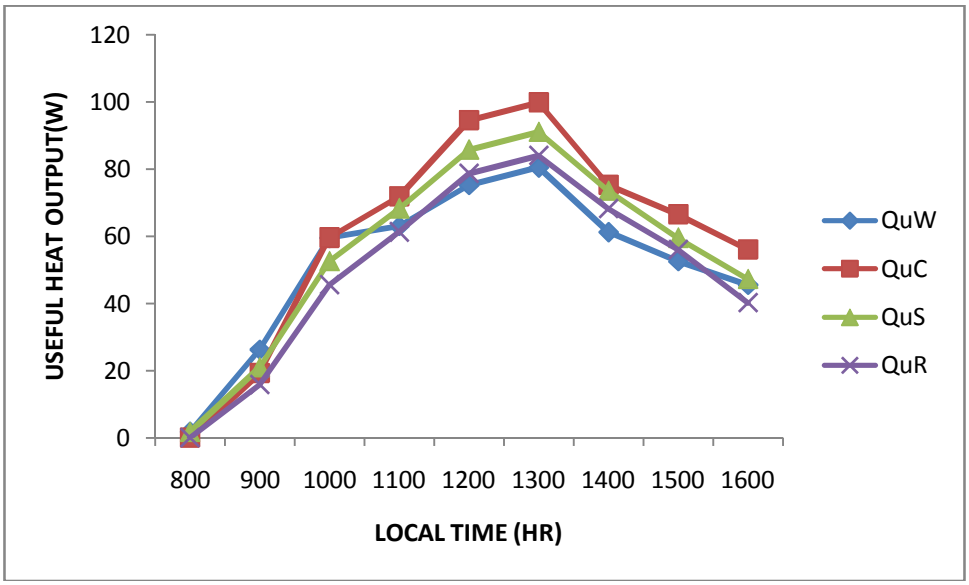


Fig 4.5: Graph of the Useful heat output against the local time for day1

Figure4.5 shows that the useful heat output is highest in the collector without honeycomb in the early hours of the day which is due to reflection losses that is more predominant in collector with honeycomb. At elevated absorber temperature (i.e. temperature more than 70^{o}C), the useful heat gain by the collectors with honeycomb was higher because the rate of convective heat losses in the collector without honeycomb was more than the reflection losses that took place in collectors with honeycomb. Therefore the useful heat output in the collector with circular cell honeycomb was the highest followed by the square cell, rectangular cell and collector without honeycomb respectively.

The thermal and exergetic efficiency of the collector is proportional to the useful heat gained.

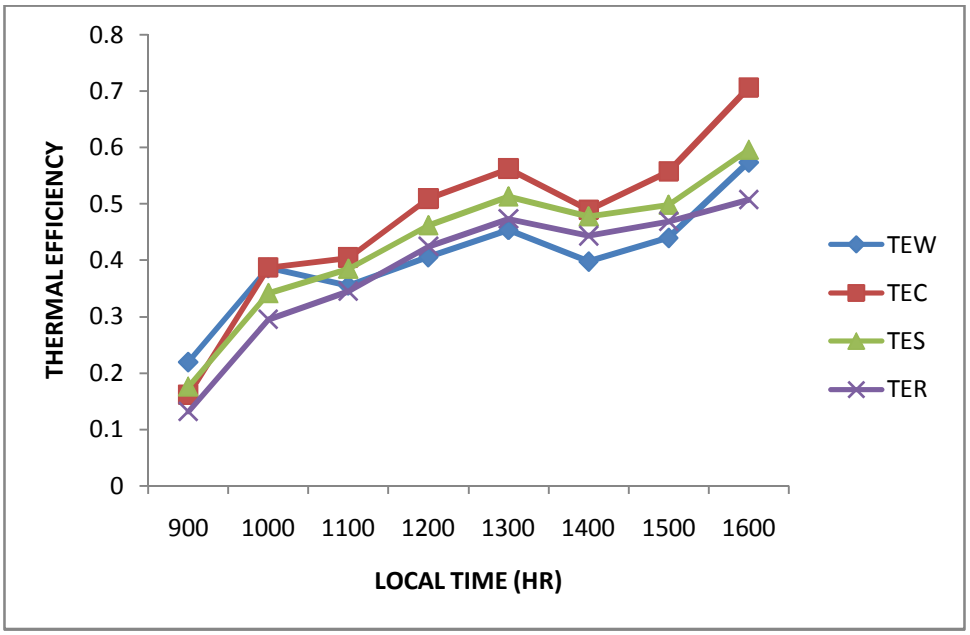


Fig 4.6: Graph of the Thermal efficiency against the local time for day1

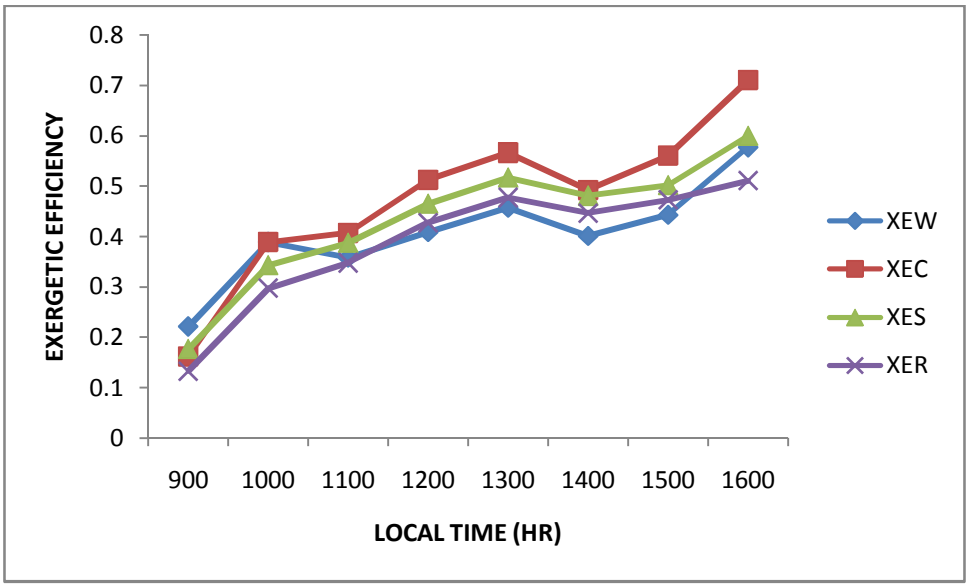


Fig 4.7: Graph of the Exergetic efficiency against the local time for day1

Figures 4.6 and 4.7 shows that collector with circular cell honeycomb has the highest thermal and exergetic efficiency followed by the square cell, rectangular cell and collector without honeycomb respectively. At noon collector without honeycomb makes use of 40.81% of

the available energy while the circular, square and rectangular cell makes use of 51.25%, 46.5%, and 42.71% of the available energy respectively. Results for day 2 and day3 are similar to those of day1. Figure4.8 to 4.13 shows the relationship between the Rayleigh number, Nusselt number, convective heat transfer coefficient, useful heat output, thermal efficiency and exergetic efficiency against the local time for circular, square and rectangular cell collector and collector without honeycomb for day2.

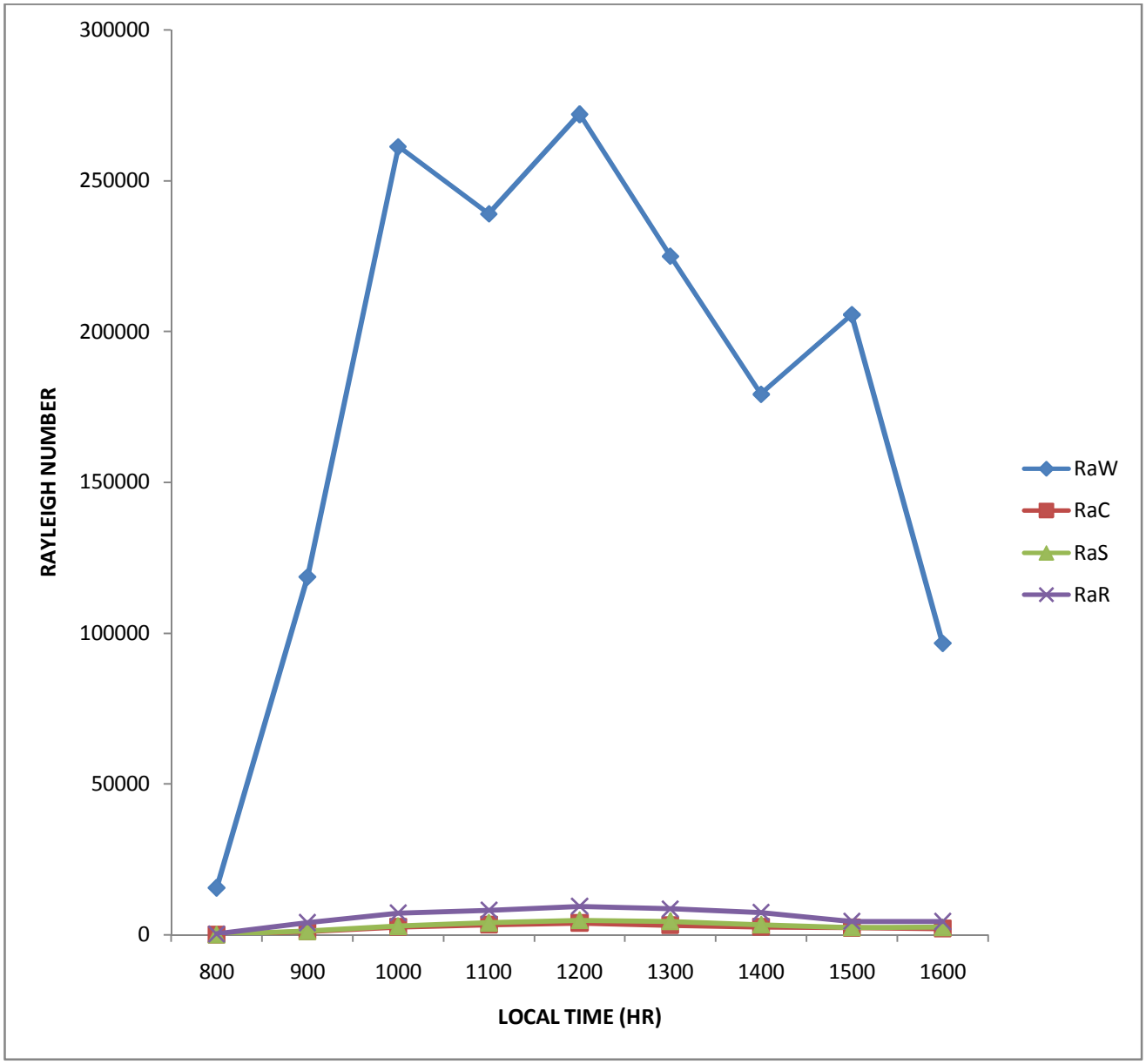


Fig 4.8: Graph of the Rayleigh number against the local time for day2

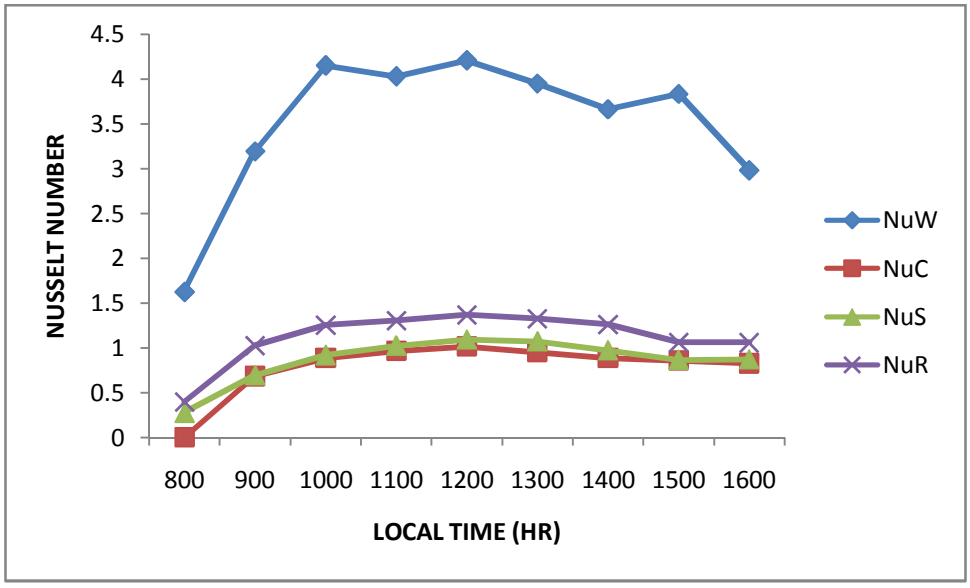


Fig 4.9: Graph of the Nusselt number against the local time for day2

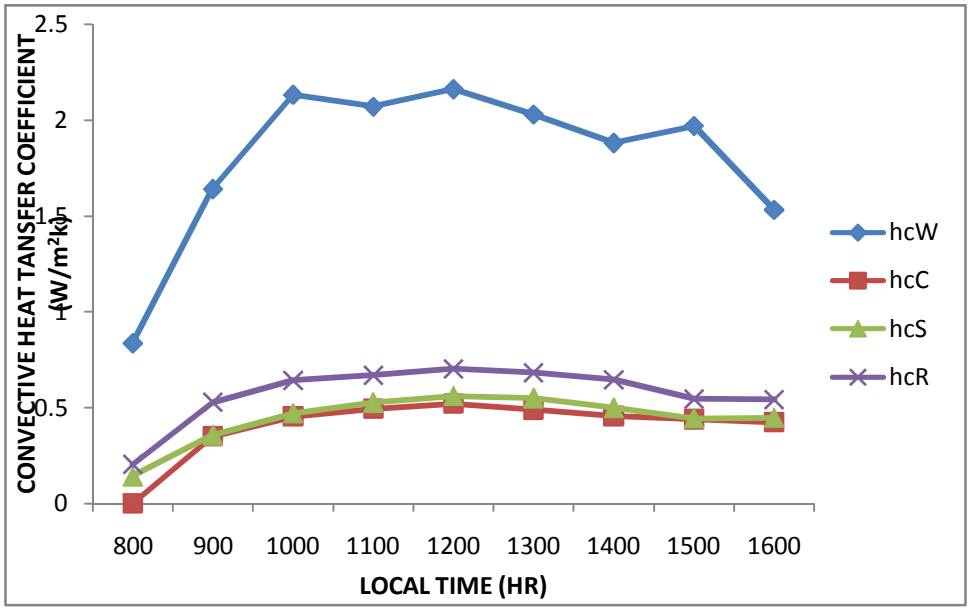


Fig 4.10: Graph of the Convective heat transfer coefficient against the local time for day2

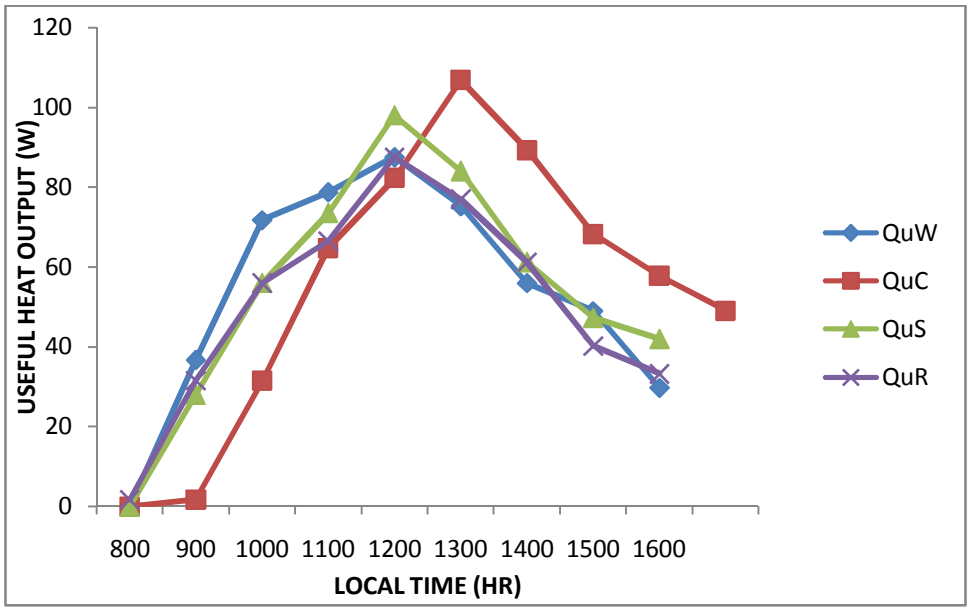


Fig 4.11: Graph of the Useful heat output against the local time for day2

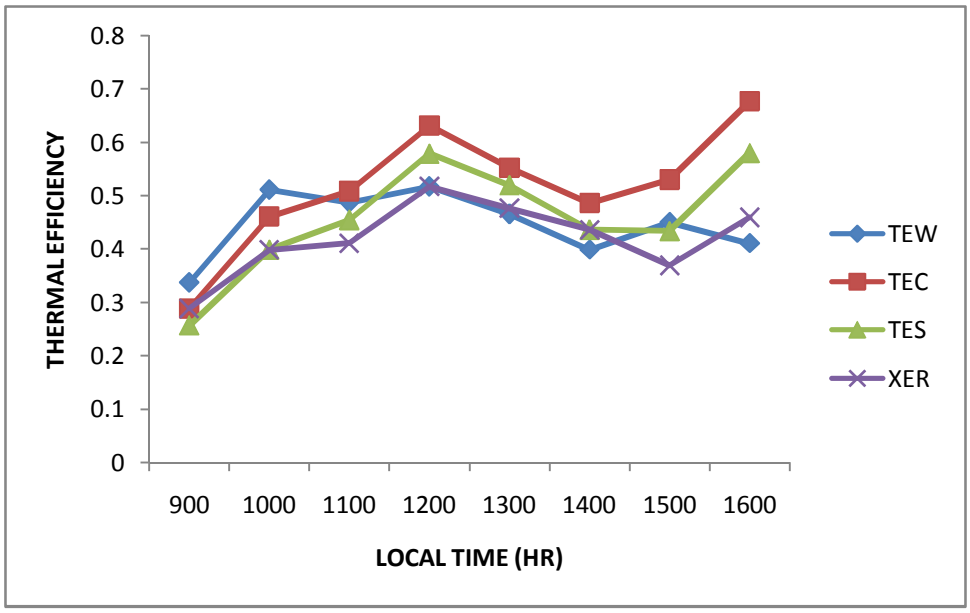


Fig 4.12: Graph of the Thermal efficiency against the local time for day2

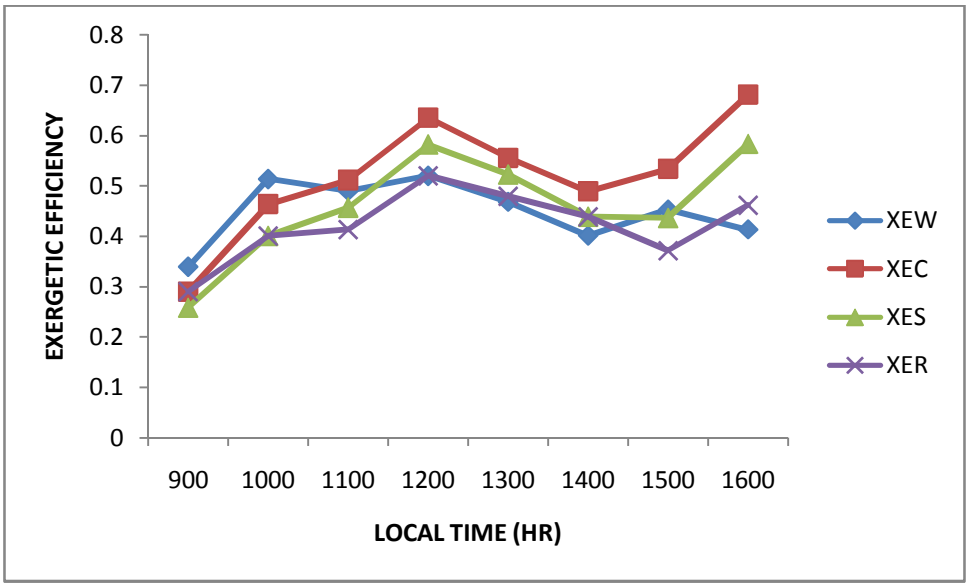


Fig 4.13: Graph of the Exergetic efficiency against the local time for day2

At noon on day2 collector without honeycomb makes use of 52% of the available energy while the circular, square and rectangular cell makes use of 63.46%, 58.24%, and 52% of the available energy respectively.

Similarly, Figure4.14 to 4.19 shows the relationship between the Rayleigh number, Nusselt number, convective heat transfer coefficient, useful heat output, and thermal efficiency and exergetic efficiency against the local time for circular, square and rectangular cell collector and collector without honeycomb for day3.

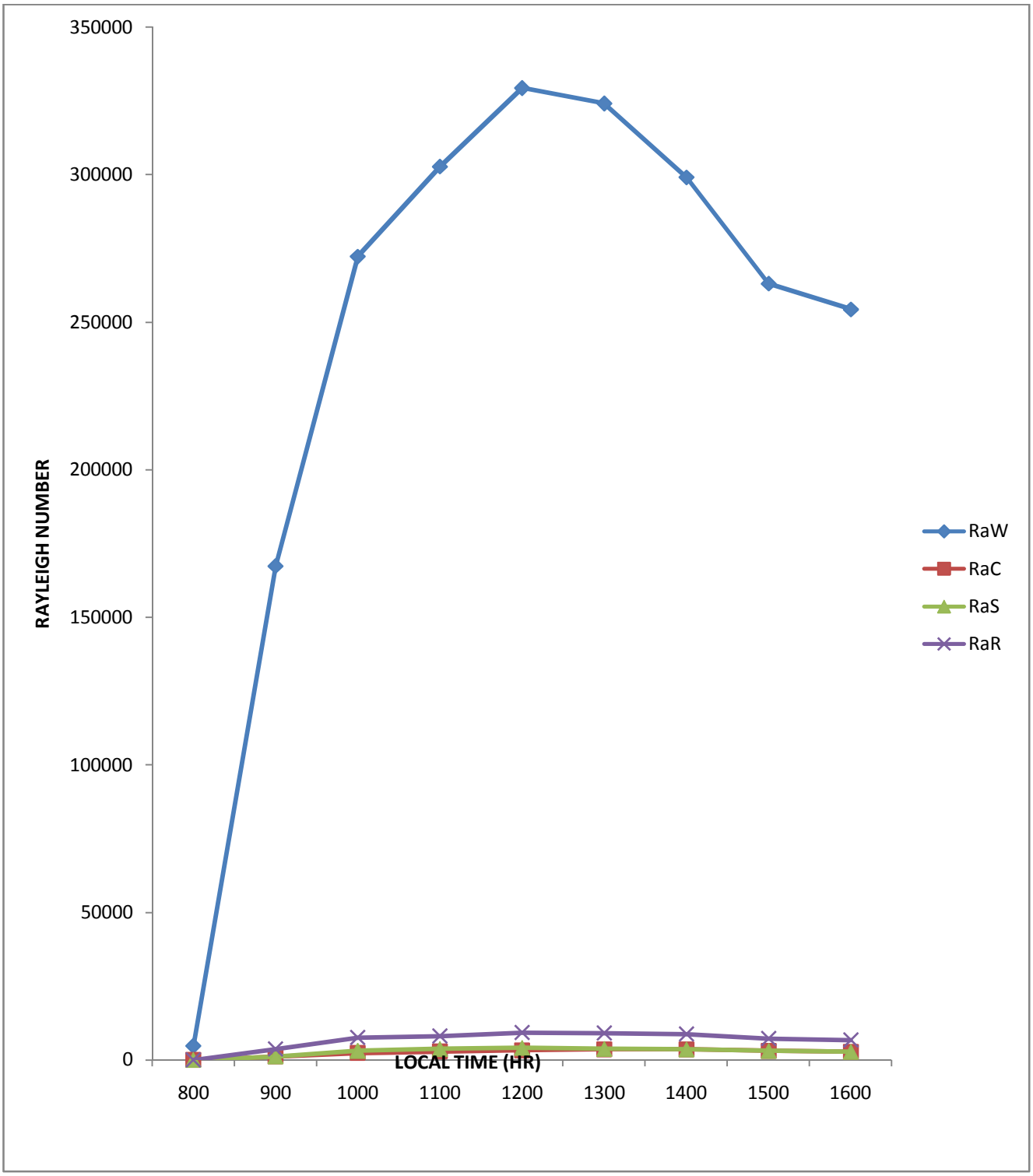


Fig 4.14: Graph of the Rayleigh number against the local time for day3

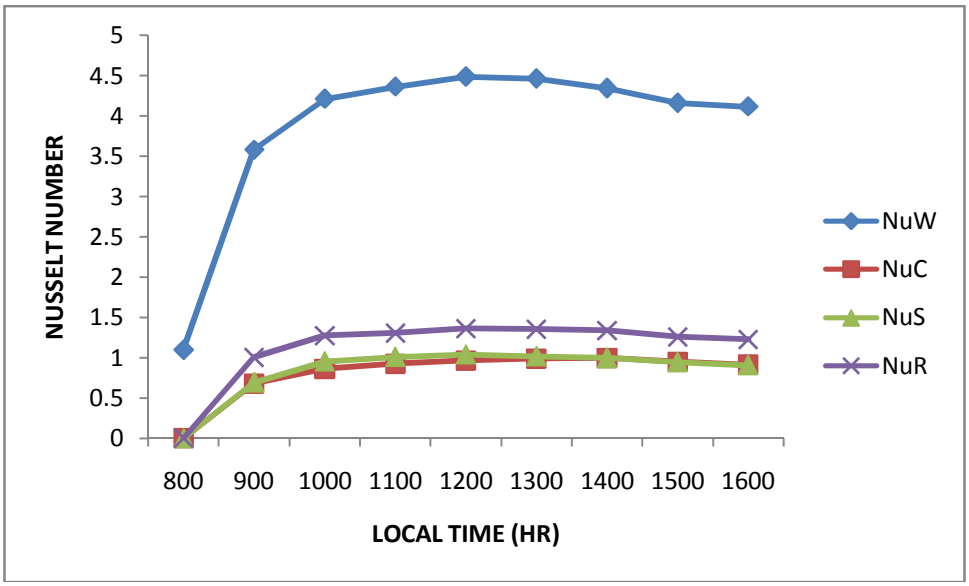


Fig 4.15: Graph of the Nusselt number against the local time for day3

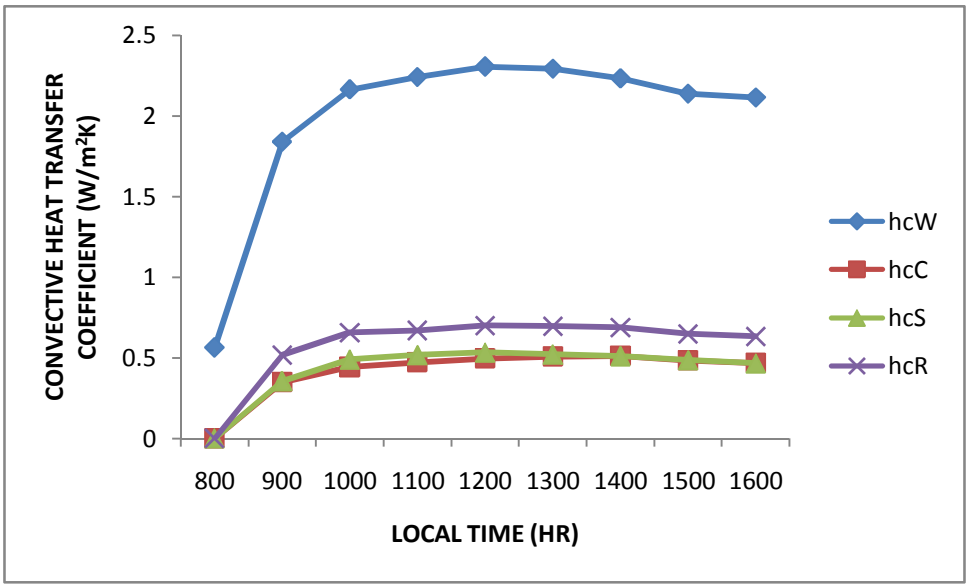


Fig 4.16: Graph of the Convective heat transfer coefficient against the local time for day3

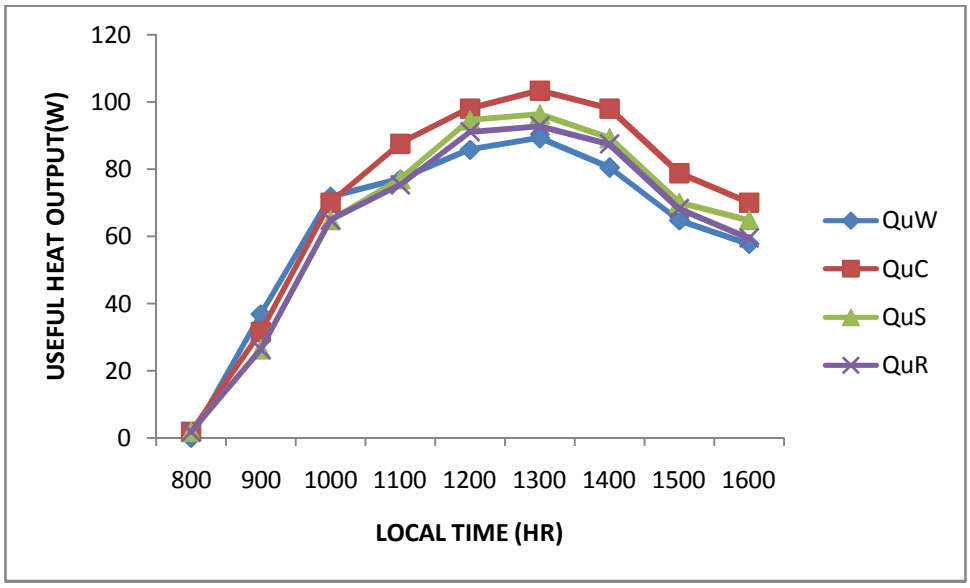


Fig 4.17: Graph of the Useful heat output against the local time for day3

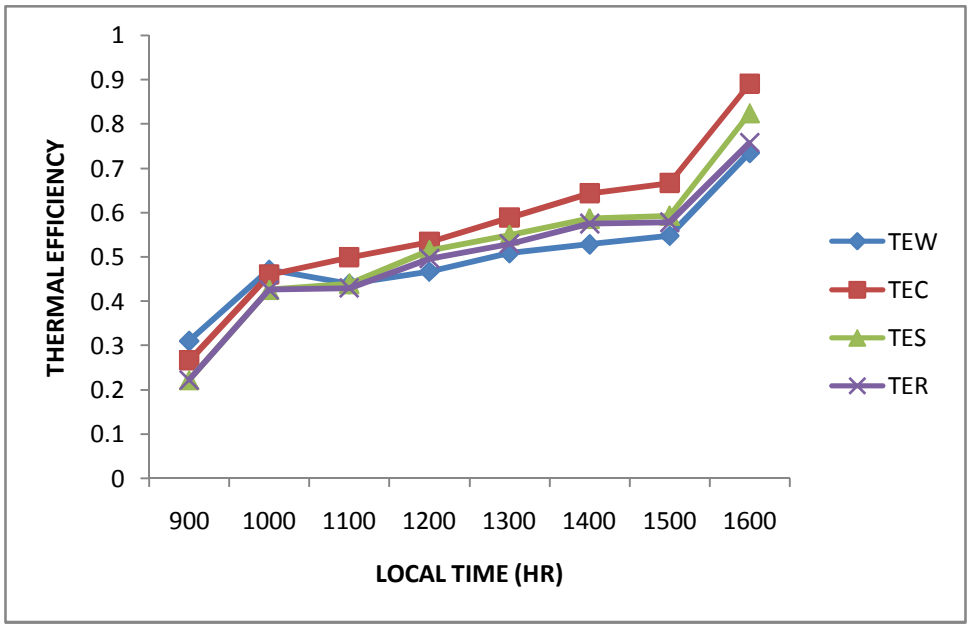


Fig 4.18: Graph of the Thermal efficiency against the local time for day3

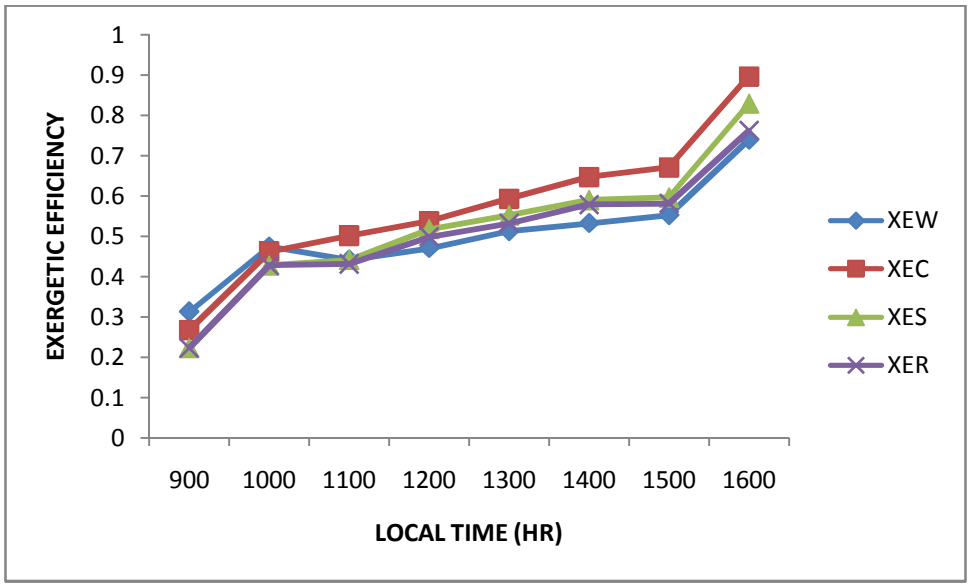


Fig 4.19: Graph of the Exergetic efficiency against the local time for day3

At noon on day3 collector without honeycomb makes use of 47% of the available energy while the circular, square and rectangular cell makes use of 53.71%, 51.79%, and 49.88% of the available energy respectively.

There is low solar insolation in most part of day4 which makes the optical losses in collector with honey comb more than the convective losses in collector without honeycomb hence, better performance of collector without honeycomb when compared with those with honeycomb as shown in figure 4.20 to 4.25 below.

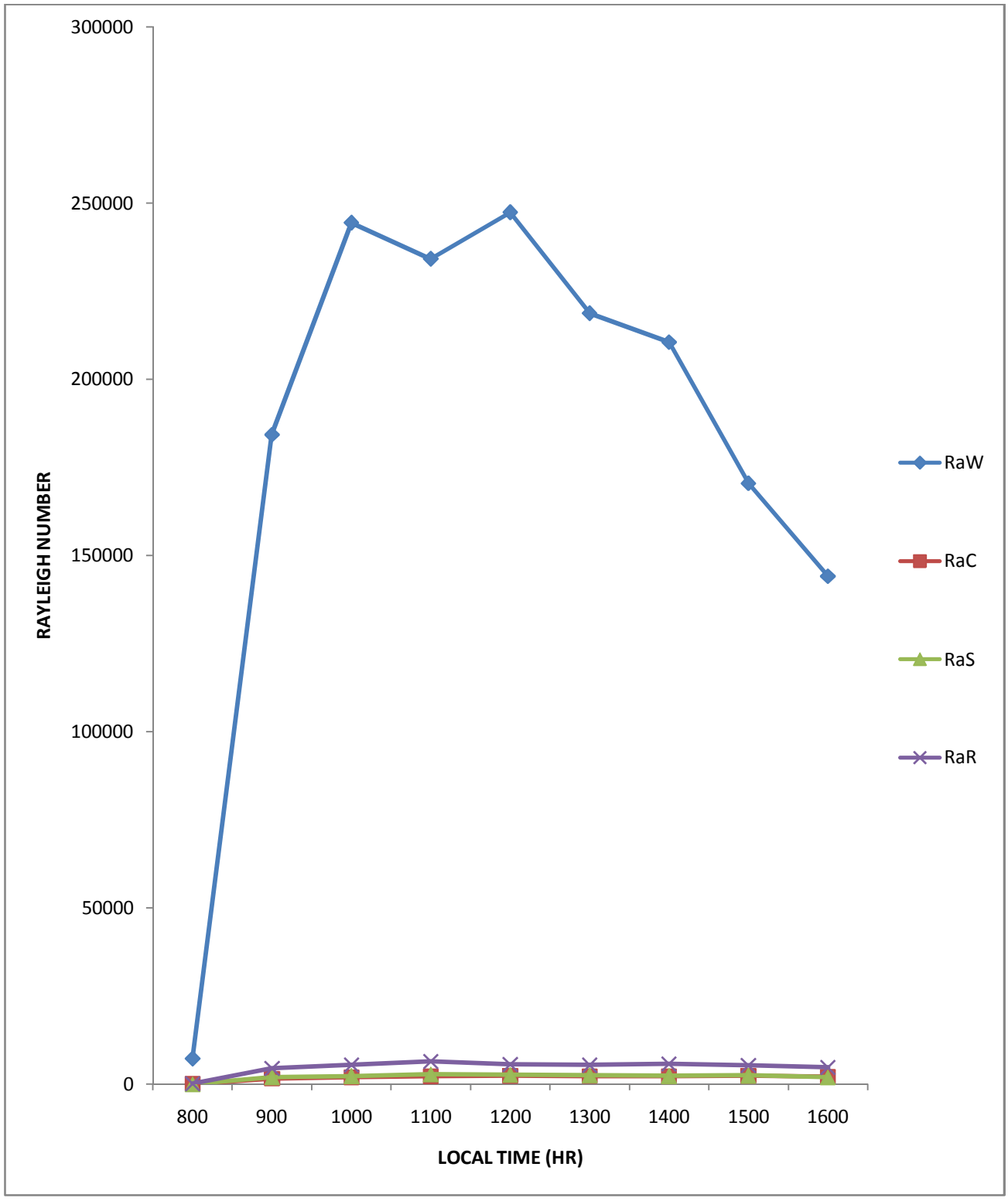


Fig 4.20: Graph of the Rayleigh number against the local time for day4

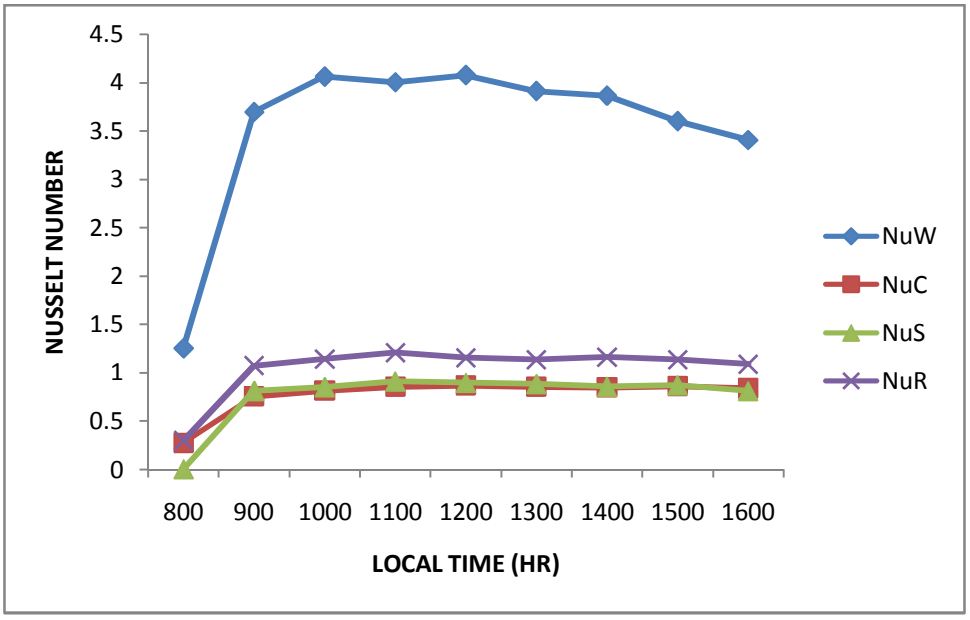


Fig 4.21: Graph of the Nusselt number against the local time for day4

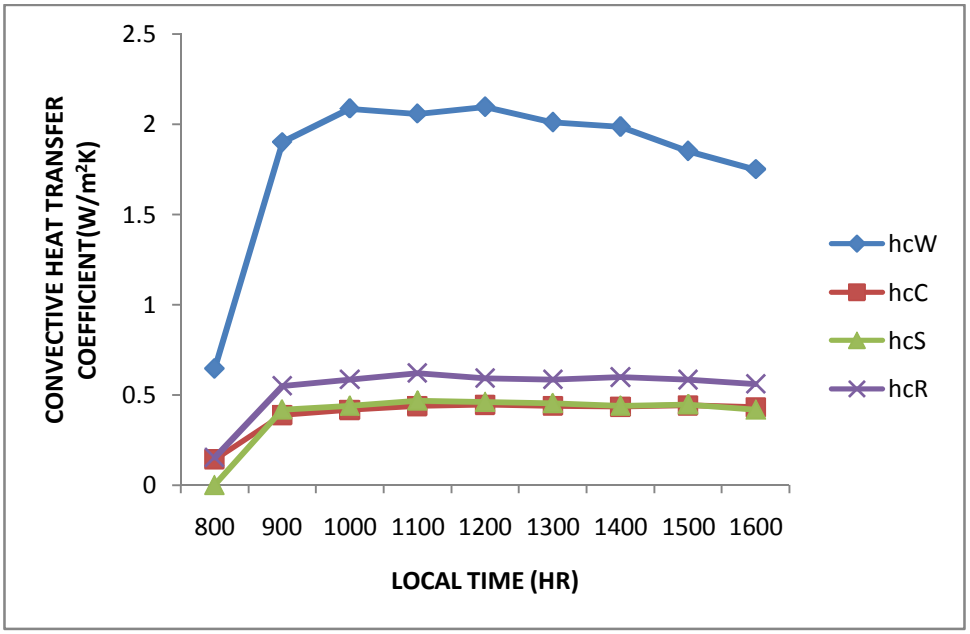


Fig 4.22: Graph of the Convective heat transfer coefficient against the local time for day4

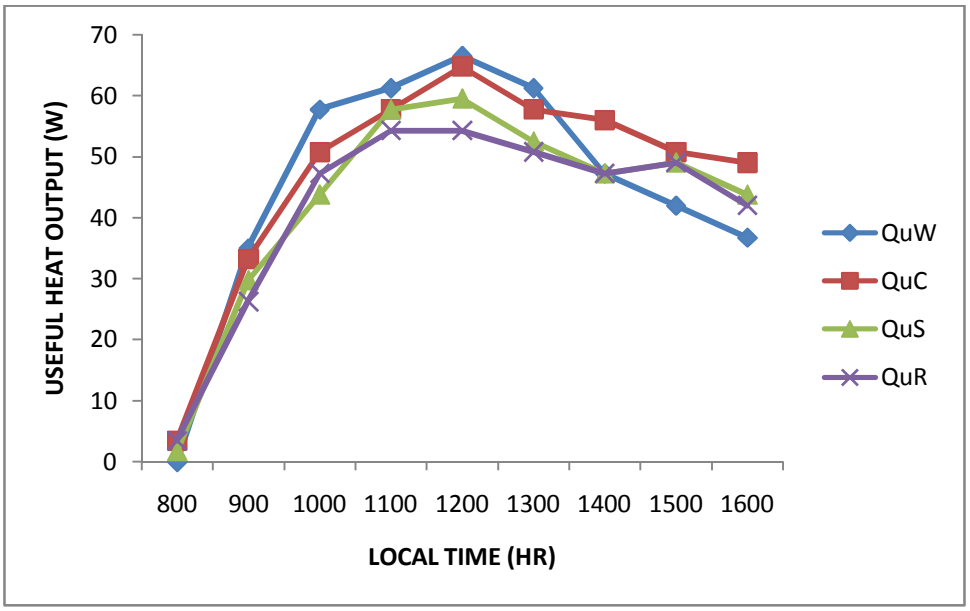


Fig 4.23: Graph of the Useful heat output against the local time for day4

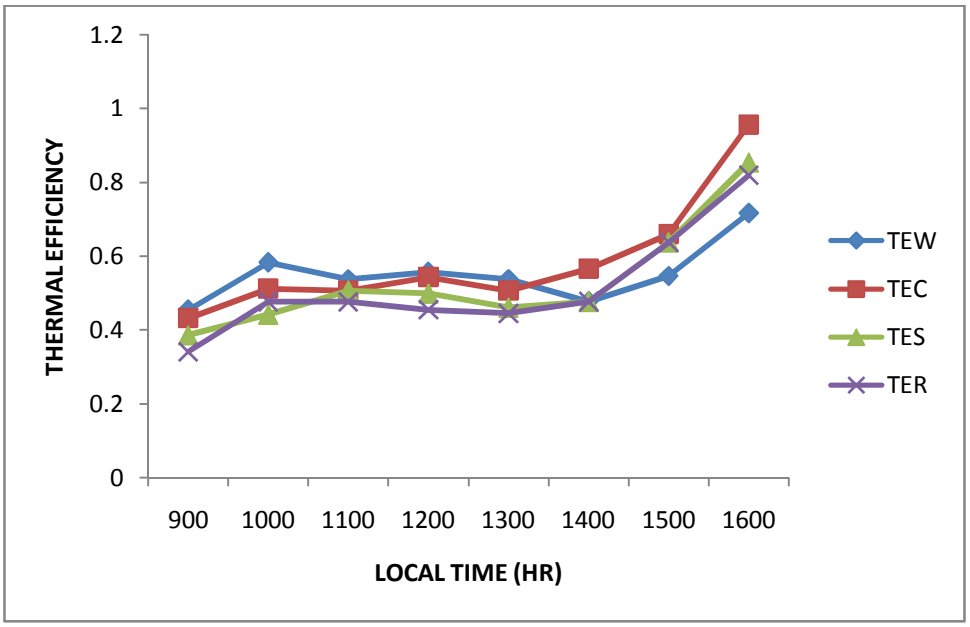


Fig 4.24: Graph of the Thermal efficiency against the local time for day4

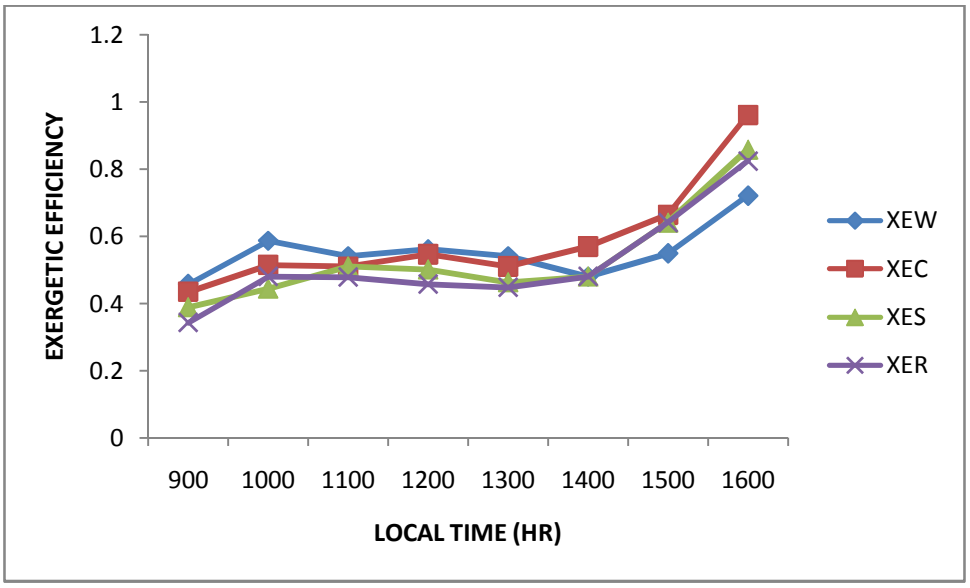


Fig 4.25: Graph of the Exergetic efficiency against the local time for day4

At noon, Collector without honeycomb makes use of 56.07% of the available energy at noon while the circular, square and rectangular cell makes use of 54.59%, 50.16%, and 45.74% of the available energy respectively.

CHAPTER FIVE

SUMMARY, CONCLUSION AND RECOMMENDATION

5.1 Summary

The research work was carried out to study the performance of square cell, circular cell and rectangular cell honey comb geometries in the suppression of convective heat transfer from the absorber plate.

Four similar flat plate solar water heaters were designed, constructed and experiments carried out in the Department of Mechanical Engineering Ahmadu Bello University Zaria between 1 and 7th of May 2009.

The water inlet and outlet temperatures as well as the ambient temperature were measured using mercury in glass thermometer while the absorber plate and cover plate temperatures were measured using thermocouples. The results were tabulated and plotted against the local time.

From the result it was observed that two fundamental losses take place from the front side of the collector are optical and convective heat losses. The optical losses which were more predominant in collectors equipped with honeycomb were as a result of multiple reflection and refraction of solar rays while the convective heat losses were a result of temperature gradient between the absorber plate and the cover glass.

On a clear day with high intensity of solar insolation the convective heat losses in collector without honeycomb were far more than the optical losses in collectors with honeycomb as observed in day1, 2 and 3. This justifies the use of honeycomb in flat plate solar collector in the tropical region and high temperature heating.

While on a cloudy day with low intensity of solar insolation. The optical losses in collector with honeycomb were more than the convective heat losses in collector without honeycomb as observed in day4. This justifies the use flat plate solar collector without honeycomb in the polar region and low temperature heating.

In summary out of the three honeycomb geometries compared, the circular cell honeycomb had best performance followed by the square cell and rectangular cell respectively. This is because for the same hydraulic diameter the rectangular cell honeycomb has highest cross sectional area followed by square and circular cell honeycomb and the air motion and convective heat loss is proportional to the cross sectional area. The narrow nature of rectangular cell honeycomb increases its shading effect thereby reducing the amount of solar insolation reaching the absorber plate.

5.2 Conclusion

Efficient use of available solar energy in flat plate solar collectors can be improved upon by suppression of the convective heat losses using the honeycomb.

Three different geometries of honeycombs had been successfully studied by the design, construction and testing of four similar solar collectors equipped with circular, square and rectangular cell honeycomb. When heating is required at moderate temperature (i.e. below $70^{o}C$) collector without honeycomb is recommended but at elevated temperature collector with circular cell honeycomb had the highest thermal and exergetic efficiency. The circular cell honeycomb collected 19.32% more energy while the square and rectangular cell honeycomb collects 9.78% and 3.0% more energy respectively when compared with collector without honeycomb. The overall analysis gave an average thermal efficiency of 47.82%, 44%and 41.26% for collector with circular, square and rectangular cell honeycomb respectively, while the collector without

honeycomb had 40.08%. Similarly, the overall analysis gave an average exergetic efficiency of 48.8%, 44.9%and 42.1% for collector with circular, and square and rectangular cell honeycomb respectively, while the collector without honeycomb has 40.9%.

5.3 Recommendation

More sophisticated means of forming the honeycomb such as glass blowing should be adopted.

Other geometries of honeycomb such as elliptical, hexagonal, triangular etc. should be investigated.

The modeling of heat transfer through the honeycomb and the performance of the collector should be carried out to determine how geometry affects performance.

Solar tracking system should be incorporated to improve on the collector performance.

REFERENCES

Abdulwahab,Ogunbiyi(1986). Design and Construction of Improved Version of Solar Water Heaters,B.Eng.Thesis.A.B.U.Zaria.

Abou-Ziyan, H.Z.and Richards, R.F. (1997).Effect of Gap Thickness on a Rectangular Cell Compound Honeycomb Collector. Journal of Solar Energy.60 (5).271-280.

Akinola, A.O. and Fapetu,o.p., (2004)Development and Performance Evaluation of a Mixed Mode Solar Food Dryer in Akure, Nigeria Journal of Engineering Applications Volume2 , No.2.Research Communications,Lagos,Nigeria.

Bala, E.J. (1980) Solar Energy Collector Design for Rural Refrigeration.M. Eng. Thesis. A.B.U. Zaria.

Buchberg,H.,Catton,I. and Edwards,D.K.,(1976)Natural Convection in Enclosed Space.A Review of application to Solar Energy Collection, Transaction of ASME
Journal of Heat Transfer.98, 193

Charters, W.W.and Guthrie, K.I. (1982).An Evaluation of a Transverse Slatted Flat Plate Collector. Journal of Solar Energy. 28(2).89-97.

Collares-perira,m. and Rabi, A., (1979) The Average Distribution of Solar Radiation-Correlations Between Diffuse and Hemispherical and Between Daily and Hourly Insolation Values, Journal of Solar Energy,22,155.

Cooper, P.I., Digital Simulation of Transient Solar Still Processes, Journal of Solar Energy, 12,313

Edwards,D.K.,Arnold,J.N. and Catton I.(1976) End Clearance Effects on Rectangular-Honeycomb Solar Collectors. Journal of Solar Energy,18,(3),

Ghoneim, A.A (2005) Performance Optimization of Solar Collector Equipped with Different Arrangement of Square Celled Honeycomb. International Journal of Thermal Sciences 44(1), 95-105.

Gupta, V.K., Tiwari, N.K. and Iyagi, H.R. (1978) Heat Transfer Analysis of Flat Plate Type Domestic Solar Water Heater. Proceeding of Solar Energy Society Congress. New Delhi, India

Herrick, O. (1985). Solar Energy Thermal Converters. Proceedings of The Workshop on The Physics and Technology of Solar Energy Conversion Held at University of Ibadan, Nigeria.

Holland's, K.G.T. (1965) Honeycomb Devices in Flat Plate Solar Collectors. Journal of Solar Energy .9(3).159-164.

Holland K.G.T.,Unny, T.E., Raaighly,G.D and Konicek, L,(1975) Free Convective Heat Transfer Across Inclined Air Layers, ASME paper75 HT55

Kay, H.K Charters, W.W.S (1978) Convection Effects in Slat Collectors Proceeding of International Solar Energy Society Congress. New Delhi, India. 965-970

Khalil, M.F. (1978) Performance of Flat Plate Solar Collectors. Proceedings of Solar Energy and Conversion Symposium, Miami, Florida, USA.74-87

McDaniels, D.K. (1979). The sun our Future Energy Source. John Wiley and Sons inc.Newyork.

Mckeigh, J.C (1978). Solar Power: An Introduction to The Applications of Solar Energy Pergamon Press. Oxford.

Meinel, A.B. and Meinel, M.P. (1976) Applied Solar Energy. Addison-Wesley Publishing Company. Arizona.

Meyer, B.A, El-Wakil, M.M. and Mitchell, J.W (1978). An Interferometric Investigation of Heat Transfer in Honeycomb Solar Collector Proceeding of International Solar Energy Society Congress. New Delhi, India

O Callagham,P.W.(1981) Design and Management of Energy Conservation .A Handbook for Energy Managers, Plant Engineers and Designers.Pergamon Press

Peter, R.H., Robert, F. and Abraham, O. (1978) Optimizing Solar Energy Systems Using Continuous Flow Control. Proceeding of International Solar Energy Society Congress. New Delhi, India

Nahar,N.M. and Gupta,M.P.(2007) Studies on Gap Spacing Between Absorber and Cover Glazing in Flat Plate Solar Collectors. International Journal of Energy Research. Volume13,issue 6.

Rai,G.D.,(2005),Solar Energy Utilization Khanna publishers.Nai Sarak Delhi

Rajput, R.K. (1999) Heat and Mass Transfer S Chand and Company New Delhi, India.

Rajput R.K. (2008) Fluid Mechanics and Hydraulic Machines S.Chand and company limited New Delhi India

Sayigh, A.A.M. (1978) A Comparison Among Various Flat plate Collectors With Honeycomb Structures. Proceeding of Solar Energy Society Congress. New Delhi, India. 924-929

Suleiman, R.B.O. (2007). Design, Modeling and Simulation of a Solar Powered Adsorption Refrigeration System. First P hD Seminar. A.B.U Zaria.

Tiwari,G.N.(2006) Solar Energy Narosa Publishing House. New Delhi.

APPENDIX I: Table of Measured Solar Data for December 2005

Date	$H_m(MJ/m^2)$	Sun shine hour
1/12/05	18.8	10.4
2/12/05	19.2	10.5
3/12/05	18.3	10.7
4/12/05	18.9	10.5
5/12/05	17.3	9.7
6/12/05	11	3.1
7/12/05	18.2	10.2
8/12/05	17.5	10.2
9/12/05	17.3	10.3
10/12/05	17.2	10.5
11/12/05	17.3	10.1
12/12/05	17.7	10.3
13/12/05	18.2	10.6
14/12/05	17.6	10.6
15/12/05	17.1	10.2
16/12/05	16.8	10.4
17/12/05	17.8	10.6
18/12/05	18.6	10.7
19/12/05	15.9	10.4
20/12/05	16.4	9.4
21/12/05	16.6	10.4
22/12/05	13.8	9.7
23/12/05	14.6	9.7
24/12/05	12.7	7
25/12/05	17.7	9.6
26/12/05	16.6	9.5
27/12/05	15.1	9.6
28/12/05	14.9	9.9
29/12/05	15.8	9.9
30/12/05	16.7	9.8
31/12/05	18.1	10.1

Source: Nigeria Metrological Agency, Nigeria College of Technology Zaria.

APPENDIX II : TABLE OF CALCULATED SOLAR PARAMETERS

s/n	N(day)	σ	W_s	$H_o(MJ/m^2)$	$H_m(MJ/m^2)$	$H_m(W/m^2)$	K_T	$H_d(W/m^2)$	$H_b(W/m^2)$	$S(W/m^2)$
1	335	-22.11	85.47	30.8	18.8	502.1	0.6096	197.3	304.8	441.2
2	336	-22.24	85.44	30.8	19.2	507.9	0.6235	186.9	321	449
3	337	-22.36	85.41	30.8	18.3	475.1	0.5952	199.4	275.7	415.6
4	338	-22.48	85.39	30.7	18.9	500	0.6156	191	309	441
5	339	-22.59	85.36	30.7	17.3	495.4	0.5642	237.3	258.1	427.9
6	340	-22.7	85.34	30.6	11	985.7	0.3592	812.9	172.8	785.4
7	341	-22.8	85.31	30.6	18.2	495.6	0.595	208.1	287.5	433.9
8	342	-22.89	85.29	30.6	17.5	476.6	0.5728	220.3	256.3	413.4
9	343	-22.97	85.27	30.5	17.3	466.6	0.5668	221.1	245.5	403.9
10	344	-23.05	85.26	30.5	17.2	455	0.564	218.1	236.9	393.4
11	345	-23.12	85.24	30.5	17.3	475.8	0.5678	224.6	251.2	412
12	346	-23.18	85.23	30.5	17.7	477.3	0.5813	212.9	264.4	416
13	347	-23.24	85.21	30.4	18.2	476.9	0.5981	197.5	279.4	418.6
14	348	-23.29	85.2	30.4	17.6	461.2	0.5788	207.9	253.3	401.5
15	349	-23.34	85.19	30.4	17.1	465.7	0.5626	224.5	241.2	402.8
16	350	-23.37	85.18	30.4	16.8	448.7	0.5529	224.8	223.9	386.4
17	351	-23.4	85.17	30.4	17.8	466.5	0.586	203.9	262.6	407.6
18	352	-23.42	85.17	30.4	18.6	482.9	0.6125	187.2	295.7	426.6
19	353	-23.44	85.17	30.4	15.9	424.7	0.5237	236.8	187.9	361
20	354	-23.45	85.16	30.4	16.4	484.6	0.5402	254.7	229.9	415
21	355	-23.45	85.16	30.4	16.6	443.4	0.5467	227.5	215.9	380.8
22	356	-23.44	85.17	30.4	13.8	395.2	0.4544	270.6	124.6	326
23	357	-23.43	85.17	30.4	14.6	418.1	0.4806	266.9	151.2	348.7
24	358	-23.41	85.17	30.4	12.7	504	0.4179	374.9	129.1	409.9
25	359	-23.39	85.18	30.4	17.7	512.2	0.5823	227.5	284.7	446.8
26	360	-23.35	85.19	30.4	16.6	485.4	0.5457	250	235.4	416.7
27	361	-23.31	85.2	30.4	15.1	436.9	0.4961	266.5	170.4	366.7
28	362	-23.27	85.2	30.5	14.9	418.1	0.4892	260.3	157.8	349.9
29	363	-23.21	85.22	30.5	15.8	443.3	0.5183	251.8	191.5	375.7
30	364	-23.15	85.23	30.5	16.7	473.4	0.5474	242.2	231.2	406.5
31	365	-23.09	85.25	30.5	18.1	497.8	0.5928	211.1	286.7	435.7

APPENDIX III: Tables of Simulated Hourly Solar Insolation for Experimental Days

Table1: Table of Solar Parameter for Experimental Days

Day	Date	$H_m(MJ/m^2)$	Sun shine hour
1	01/05/2009	19.4	9
2	02/05/2009	17.7	9
3	03/05/2009	19.2	7.9
4	06/05/2009	12.5	9.3

Source: Nigeria Metrological Agency, Nigeria College of Technology Zaria.

Table2: Simulated Hourly Solar Insolation for Day1

Time(hr)	Ω	R	I
06:00	-90	0.004265	5.746
07:00	-75	0.02951	39.76
08:00	-60	0.05889	79.34
09:00	-45	0.08863	119.4
10:00	-30	0.1143	154
11:00	-15	0.1316	177.4
12:00	0	0.1378	185.6
13:00	15	0.1316	177.4
14:00	30	0.1143	154
15:00	45	0.08863	119.4
16:00	60	0.05889	79.34
17:00	75	0.02951	39.76
18:00	90	0.004265	5.746

Table3: Simulated Hourly Solar Insolation for Day2

Time(hr)	Ω	R	I
06:00	-90	0.004354	5.352
07:00	-75	0.02958	36.36
08:00	-60	0.05893	72.43
09:00	-45	0.08863	108.9
10:00	-30	0.1142	140.4
11:00	-15	0.1316	161.7
12:00	0	0.1377	169.3
13:00	15	0.1316	161.7
14:00	30	0.1142	140.4
15:00	45	0.08863	108.9
16:00	60	0.05893	72.43
17:00	75	0.02958	36.36
18:00	90	0.004354	5.352

Table4: Simulated Hourly Solar Insolation for Day3

Time(hr)	Ω	R	I
06:00	-90	0.004441	5.922
07:00	-75	0.02965	39.54
08:00	-60	0.05897	78.62
09:00	-45	0.08862	118.2
10:00	-30	0.1142	152.2
11:00	-15	0.1315	175.3
12:00	0	0.1376	183.5
13:00	15	0.1315	175.3
14:00	30	0.1142	152.2
15:00	45	0.08862	118.2
16:00	60	0.05897	78.62
17:00	75	0.02965	39.54
18:00	90	0.004441	5.922

Table5: Simulated Hourly Solar Insolation for Day4

Time(hr)	Ω	R	I
06:00	-90	0.004696	4.076
07:00	-75	0.02985	25.91
08:00	-60	0.05907	51.28
09:00	-45	0.08861	76.92
10:00	-30	0.1141	99.01
11:00	-15	0.1313	114
12:00	0	0.1374	119.3
13:00	15	0.1313	114
14:00	30	0.1141	99.01
15:00	45	0.08861	76.92
16:00	60	0.05907	51.28
17:00	75	0.02985	25.91
18:00	90	0.004696	4.076

APPENDIX IV: TABLES OF EXPERIMENTAL RESULT

DAY1(01/05/09)

Table 1:Result for collector without honeycomb

TIME	T_1	T_2	T_p	T_c	T_a	Ra	Nu	h_c	Q_u	TE	XE	X_{en}
800	31	32	32	32	29	0	0	0	1.75	0.02206	0.02217	78.93
900	33	48	51.6	39.7	31	136909	3.348	1.721	26.25	0.2198	0.221	118.8
1000	36	70	74.4	50.6	32	260066	4.146	2.131	59.5	0.3866	0.3887	153.1
1100	38	74	75.9	58.3	34	189716	3.732	1.918	63	0.3552	0.3573	176.3
1200	40	83	85.6	70.3	38	159825	3.525	1.812	75.25	0.4054	0.4081	184.4
1300	41	87	89.1	72.6	38	170948	3.605	1.853	80.5	0.4539	0.4569	176.2
1400	42	77	79.8	67.4	38	131157	3.3	1.696	61.25	0.3979	0.4006	152.9
1500	41	71	72.8	61.8	37	118503	3.19	1.64	52.5	0.4397	0.4425	118.6
1600	39	65	66.8	53.7	34	144112	3.405	1.75	45.5	0.5736	0.577	78.86

Table 2:Result for collector with circular cell honeycomb

TIME	T_1	T_2	T_p	T_c	T_a	Ra	Nu	h_c	Q_u	TE	XE	X_{en}
800	30	30	31.2	31	29	19.29	0.1742	0.08954	0	0	0	78.93
900	32	43	46.8	37.6	31	856	0.6167	0.317	19.25	0.1612	0.1621	118.8
1000	33	67	69.2	43.3	32	2307	0.8583	0.4412	59.5	0.3866	0.3887	153.1
1100	35	76	78.8	49.2	34	2576	0.8904	0.4577	71.75	0.4046	0.407	176.3
1200	36	90	91.6	53.7	38	3216	0.9587	0.4928	94.5	0.5091	0.5125	184.4
1300	39	96	97.2	58	38	3279	0.965	0.496	99.75	0.5624	0.5662	176.2
1400	40	83	85.1	51.4	38	2896	0.9259	0.4759	75.25	0.4889	0.4921	152.9
1500	38	76	78.2	48.6	37	2581	0.8909	0.4579	66.5	0.557	0.5605	118.6
1600	37	69	70.9	44.1	34	2378	0.867	0.4456	56	0.706	0.7101	78.86

Table 3:Result for collector with square cell honeycomb

TIME	T_1	T_2	T_p	T_c	T_a	Ra	Nu	h_c	Q_u	TE	XE	X_{en}
800	30	31	32	31	29	128.2	0.3275	0.1683	1.75	0.02206	0.02217	78.93
900	33	45	47.4	36.3	31	1376	0.7225	0.3714	21	0.1759	0.1768	118.8
1000	33	63	66.7	41.7	32	2983	0.935	0.4806	52.5	0.3411	0.343	153.1
1100	35	74	76.5	50.3	34	3040	0.941	0.4837	68.25	0.3848	0.3871	176.3
1200	37	86	88.3	58.6	38	3346	0.9716	0.4994	85.75	0.462	0.465	184.4
1300	39	91	92.6	59.9	38	3655	1.001	0.5143	91	0.5131	0.5165	176.2
1400	40	82	85.4	53.7	38	3612	0.9966	0.5123	73.5	0.4775	0.4807	152.9
1500	39	73	75.6	48.2	37	3194	0.9565	0.4917	59.5	0.4983	0.5015	118.6
1600	37	64	66.9	43.2	34	2820	0.9177	0.4717	47.25	0.5957	0.5992	78.86

Table 4:Result for collector with rectangular cell honeycomb

TIME	T_1	T_2	T_p	T_c	T_a	Ra	Nu	h_c	Q_u	TE	XE	X_{en}
800	31	31	31.8	31.4	29	130	0.329	0.1691	0	0	0	78.93
900	33	42	45.6	37.1	31	2677	0.9018	0.4635	15.75	0.1319	0.1326	118.8
1000	35	61	63.8	40.7	32	7030	1.244	0.6396	45.5	0.2956	0.2972	153.1
1100	38	73	77.3	51.6	34	7539	1.274	0.6546	61.25	0.3454	0.3474	176.3
1200	40	85	88.1	59.4	38	8193	1.309	0.673	78.75	0.4242	0.4271	184.4
1300	41	89	91.5	62.5	38	8201	1.31	0.6733	84	0.4736	0.4768	176.2
1400	41	80	82.4	54.8	38	7997	1.299	0.6677	68.25	0.4434	0.4463	152.9
1500	40	72	73.6	47.3	37	7807	1.289	0.6623	56	0.469	0.472	118.6
1600	38	61	62.8	41.9	34	6359	1.203	0.6185	40.25	0.5074	0.5104	78.86

DAY2(02/05/09) Table 5:Result for collector without honeycomb

TIME	T_1	T_2	T_p	T_c	T_a	Ra	Nu	h_c	Q_u	TE	XE	X_{en}
800	31	31	32.8	31.5	29	15618	1.624	0.8345	0	0	1.26E-29	72.06
900	32	53	56.7	46.2	29	118642	3.192	1.641	36.75	0.3374	0.3391	108.4
1000	33	74	77.2	53.1	30	261280	4.152	2.134	71.75	0.511	0.5137	139.7
1100	34	79	81.8	59.4	31	238998	4.031	2.072	78.75	0.487	0.4896	160.8
1200	35	85	87.6	61.8	33	272028	4.209	2.163	87.5	0.517	0.52	168.3
1300	36	79	81.4	60.3	36	224963	3.95	2.031	75.25	0.4654	0.4683	160.7
1400	37	69	70.7	54.3	35	179205	3.662	1.882	56	0.3989	0.4013	139.5
1500	36	64	66.1	47.6	34	205615	3.834	1.971	49	0.4499	0.4525	108.3
1600	35	52	53.6	45.1	32	96670	2.981	1.532	29.75	0.4108	0.4131	72.02

Table 6:Result for collector with circular cell honeycomb

TIME	T_1	T_2	T_p	T_c	T_a	Ra	Nu	h_c	Q_u	TE	XE	X_{en}
800	30	31	32.6	32.6	29	0	0	0	1.75	0.02416	0.02428	72.06
900	30	48	49.6	37.1	29	1159	0.6823	0.3507	31.5	0.2892	0.2906	108.4
1000	31	68	71.3	42.8	30	2533	0.8854	0.4551	64.75	0.4612	0.4636	139.7
1100	32	79	82.7	45.4	31	3246	0.9617	0.4943	82.25	0.5087	0.5114	160.8
1200	33	94	95.1	50.3	33	3801	1.014	0.521	106.8	0.631	0.6346	168.3
1300	35	86	89.4	52.4	36	3155	0.9527	0.4897	89.25	0.5519	0.5554	160.7
1400	34	73	75.5	46.5	35	2546	0.887	0.4559	68.25	0.4861	0.4891	139.5
1500	34	67	69.2	43.6	34	2279	0.8548	0.4394	57.75	0.5302	0.5333	108.3
1600	33	61	62.8	40.1	32	2052	0.8254	0.4243	49	0.6766	0.6803	72.02

Table 7:Result for collector with square cell honeycomb

TIME	T_1	T_2	T_p	T_c	T_a	Ra	Nu	h_c	Q_u	TE	XE	X_{en}
800	30	30	31.2	30.6	29	77.07	0.2764	0.1421	0	0	1.26E-29	72.06
900	31	47	48.3	38.4	29	1222	0.6944	0.3569	28	0.2571	0.2584	108.4
1000	31	63	65.4	41.8	30	2821	0.9178	0.4717	56	0.3989	0.4009	139.7
1100	32	74	77.1	43.6	31	3923	1.024	0.5265	73.5	0.4545	0.457	160.8
1200	33	89	90.4	48.7	33	4752	1.092	0.5613	98	0.579	0.5824	168.3
1300	35	83	85.3	46.5	36	4469	1.07	0.5499	84	0.5195	0.5227	160.7
1400	35	70	72.6	44.2	35	3345	0.9714	0.4993	61.25	0.4363	0.4389	139.5
1500	34	61	62.5	42.7	34	2374	0.8665	0.4454	47.25	0.4338	0.4364	108.3
1600	34	58	59.8	39.7	32	2431	0.8734	0.4489	42	0.5799	0.5831	72.02

Table 8:Result for collector with rectangular cell honeycomb

TIME	T_1	T_2	T_p	T_c	T_a	Ra	Nu	h_c	Q_u	TE	XE	X_{en}
800	30	31	32.1	31.4	29	227.4	0.3964	0.2038	1.75	0.02416	0.02428	72.06
900	32	50	53.6	40.8	29	3957	1.027	0.5281	31.5	0.2892	0.2906	108.4
1000	32	64	66.2	42.5	30	7166	1.252	0.6437	56	0.3989	0.4009	139.7
1100	34	72	73.8	46.7	31	8049	1.302	0.6691	66.5	0.4113	0.4135	160.8
1200	34	84	85.9	53.6	33	9328	1.367	0.7028	87.5	0.517	0.52	168.3
1300	36	80	81.6	52.4	36	8501	1.326	0.6814	77	0.4762	0.4792	160.7
1400	36	71	73.1	48.5	35	7295	1.26	0.6475	61.25	0.4363	0.4389	139.5
1500	35	58	59.8	45.4	34	4378	1.063	0.5462	40.25	0.3695	0.3717	108.3
1600	35	54	55.7	41.7	32	4308	1.057	0.5432	33.25	0.4591	0.4617	72.02

DAY3(03/05/09) Table 9:Result for collector without honeycomb

Time	T1	T2	Ta	Tc	Tp	Hc	Nu	Qu	Ra	TE	XE	Xen
800	30	30	28	30.5	30.9	0.5643	1.098	0	4829	0	0.00E+00	78.22
900	31	52	29	41.6	56.3	1.84	3.58	36.75	167389	0.311	0.3126	117.6
1000	32	73	30	53.7	78.9	2.164	4.21	71.75	272280	0.4713	0.4738	151.4
1100	33	77	31	54.4	82.6	2.242	4.361	77	302731	0.4392	0.4416	174.4
1200	33	82	33	55.5	86.4	2.306	4.486	85.75	329353	0.4673	0.47	182.5
1300	35	86	34	58.9	89.6	2.293	4.462	89.25	324112	0.5091	0.5121	174.3
1400	36	82	35	56.2	84.2	2.233	4.344	80.5	299095	0.5288	0.532	151.3
1500	35	72	36	52.1	76.3	2.139	4.162	64.75	263103	0.548	0.5515	117.4
1600	34	67	35	48.4	71.5	2.115	4.115	57.75	254350	0.7347	0.7392	78.12

Table 10:Result for collector with circular cell honeycomb

Time	T1	T2	Ta	Tc	Tp	Hc	Nu	Ra	Qu	TE	XE	Xen
800	29	30	28	31.5	31.5	0	0	0	1.75	0.02226	0.02237	78.22
900	29	47	29	40.3	52.7	0.3486	0.6782	1138	31.5	0.2666	0.268	117.6
1000	30	70	30	48.6	75.1	0.442	0.86	2321	70	0.4598	0.4622	151.4
1100	31	81	31	51.2	84.3	0.4733	0.9208	2849	87.5	0.4991	0.5018	174.4
1200	33	89	33	54.9	93.4	0.4947	0.9624	3253	98	0.5341	0.5371	182.5
1300	34	93	34	56.5	98.5	0.5076	0.9875	3514	103.3	0.5892	0.5927	174.3
1400	34	90	35	52.3	94.7	0.5112	0.9945	3589	98	0.6438	0.6477	151.3
1500	33	78	36	48.4	83.9	0.4852	0.944	3070	78.75	0.6665	0.6707	117.4
1600	33	73	35	47.5	79.2	0.4685	0.9116	2764	70	0.8906	0.896	78.12

Table 11:Result for collector with square cell honeycomb

Time	T1	T2	Ta	Tc	Tp	hc	Nu	Ra	Qu	TE	XE	Xen
800	29	30	28	31	31	0	0	0	1.75	0.02226	0.02237	78.22
900	30	45	29	39.6	49.5	0.3565	0.6935	1217	26.25	0.2222	0.2233	117.6
1000	30	67	30	44.2	70.8	0.489	0.9513	3142	64.75	0.4254	0.4276	151.4
1100	32	76	31	48.1	80.1	0.5166	1.005	3706	77	0.4392	0.4416	174.4
1200	33	87	33	56.2	92.6	0.5339	1.039	4090	94.5	0.515	0.5179	182.5
1300	35	90	34	60.4	94.4	0.5204	1.013	3788	96.25	0.549	0.5522	174.3
1400	34	85	35	55.7	87.5	0.5118	0.9957	3602	89.25	0.5863	0.5899	151.3
1500	34	74	36	53.4	80.2	0.4857	0.9449	3079	70	0.5925	0.5962	117.4
1600	33	70	35	51.8	75.3	0.4664	0.9073	2726	64.75	0.8238	0.8288	78.12

Table 12:Result for collector with rectangular cell honeycomb

Time	T1	T2	Ta	Tc	Tp	hc	Nu	Qu	Ra	TE	XE	Xen
800	30	31	28	30.8	30.8	0	0	1.75	0	0.02226	0.02237	78.22
900	31	46	29	38.4	50.3	0.5169	1.006	26.25	3712	0.2222	0.2233	117.6
1000	31	68	30	47.1	72.7	0.6567	1.278	64.75	7612	0.4254	0.4276	151.4
1100	32	75	31	51.8	79.5	0.6704	1.304	75.25	8096	0.4292	0.4315	174.4
1200	33	85	33	56.4	88.6	0.7002	1.362	91	9225	0.4959	0.4988	182.5
1300	35	88	34	61.3	93.3	0.6955	1.353	92.75	9042	0.529	0.5321	174.3
1500	34	73	36	54.6	79.6	0.6469	1.259	68.25	7276	0.5777	0.5813	117.4
1600	34	68	35	49.5	72.3	0.6312	1.228	59.5	6759	0.757	0.7616	78.12

DAY4(06/05/09) Table 13:Result for collector without honeycomb

Time	T1	T2	Tp	Tc	Ta	Ra	Nu	hc	Qu	TE	XE	Xen
800	31	31	32.4	31.8	27	7210	1.255	0.645	0	0	3.16E-30	51.04
900	32	52	55.5	39.4	27	184189	3.696	1.9	35	0.4551	0.4573	76.54
1000	32	65	69.6	47.5	28	244367	4.061	2.087	57.75	0.5833	0.5862	98.52
1100	33	68	72.8	51.4	31	234120	4.003	2.058	61.25	0.5375	0.5404	113.3
1200	33	71	76.4	53.6	31	247296	4.077	2.096	66.5	0.5577	0.5607	118.6
1300	34	69	72.3	52.3	32	218673	3.913	2.011	61.25	0.5375	0.5405	113.3
1400	34	61	65.7	46.8	31	210443	3.864	1.986	47.25	0.4773	0.4798	98.47
1500	33	57	59.4	44.3	30	170409	3.601	1.851	42	0.5462	0.549	76.5
1600	32	53	56.6	43.9	31	144034	3.405	1.75	36.75	0.7167	0.7206	51

Table14:Result for collector with circular cell honeycomb

Time	T1	T2	Tp	Tc	Ta	Ra	Nu	hc	Qu	TE	XE	Xen
800	30	32	32.6	31.8	27	76.88	0.2762	0.142	3.5	0.06826	0.06858	51.04
900	30	49	54.3	37.1	27	1583	0.757	0.3891	33.25	0.4324	0.4344	76.54
1000	31	60	63.4	41.6	28	1964	0.8135	0.4181	50.75	0.5126	0.5151	98.52
1100	32	65	67.8	42.4	31	2270	0.8537	0.4388	57.75	0.5068	0.5095	113.3
1200	32	69	73.1	46.1	31	2381	0.8673	0.4458	64.75	0.543	0.5459	118.6
1300	33	66	69.6	43.8	32	2295	0.8568	0.4404	57.75	0.5068	0.5096	113.3
1400	32	64	68.2	43.4	31	2212	0.8463	0.435	56	0.5657	0.5687	98.47
1500	32	61	66.4	40.6	30	2318	0.8596	0.4418	50.75	0.6599	0.6634	76.5
1600	31	59	62.2	38.5	31	2150	0.8383	0.4309	49	0.9556	0.9608	51

Table 15:Result for collector with square cell honeycomb

Time	T1	T2	Tp	Tc	Ta	Ra	Nu	hc	Qu	TE	XE	Xen
800	30	31	31.8	31.8	27	0	0	0	1.75	0.03413	0.03429	51.04
900	30	47	52.4	36.4	27	1968	0.814	0.4184	29.75	0.3869	0.3887	76.54
1000	31	56	59.3	40.5	28	2273	0.854	0.439	43.75	0.4419	0.4441	98.52
1100	31	64	66.8	43.6	31	2759	0.9111	0.4683	57.75	0.5068	0.5095	113.3
1200	32	66	70.9	48.3	31	2652	0.8991	0.4622	59.5	0.499	0.5016	118.6
1300	33	63	65.4	44.2	32	2525	0.8844	0.4546	52.5	0.4607	0.4633	113.3
1400	33	60	64.1	44.9	31	2289	0.856	0.44	47.25	0.4773	0.4798	98.47
1500	32	60	63.6	43.3	30	2427	0.8729	0.4487	49	0.6372	0.6405	76.5
1600	32	57	61.2	44.8	31	1964	0.8134	0.4181	43.75	0.8532	0.8578	51

Table16:Result for collector with rectangular cell honeycomb

Time	T1	T2	Tp	Tc	Ta	Ra	Nu	hc	Qu	TE	XE	Xen
800	30	32	32.8	32.5	27	97.15	0.2986	0.1535	3.5	0.06826	0.06858	51.04
900	31	46	50.6	36.2	27	4505	1.073	0.5514	26.25	0.3414	0.343	76.54
1000	31	58	60.3	42.6	28	5400	1.14	0.5857	47.25	0.4773	0.4796	98.52
1100	32	63	67.8	46.3	31	6448	1.209	0.6214	54.25	0.4761	0.4787	113.3
1200	33	64	68.4	49.5	31	5636	1.156	0.5941	54.25	0.4549	0.4574	118.6
1300	34	63	64.7	46.8	32	5390	1.139	0.5854	50.75	0.4454	0.4479	113.3
1400	34	61	63.1	44.1	31	5758	1.164	0.5984	47.25	0.4773	0.4798	98.47
1500	33	61	62.3	44.6	30	5367	1.137	0.5845	49	0.6372	0.6405	76.5
1600	32	56	58.4	42.9	31	4740	1.091	0.5608	42	0.8191	0.8235	51